Cortical representation of fear learning

Inauguraldissertation

zur

Erlangung der Würde eines Doktors der Philosophie

vorgelegt der

Philosophisch-Naturwissenschaftlichen Fakultät

der Universität Basel

von

Elisabeth Martha Maria Meyer

aus Weil der Stadt, Deutschland

Basel, 2017

Genehmigt von der Philosophisch-Naturwissenschaftlichen Fakultät

auf Antrag von:

Prof. Dr. Andreas Lüthi

(Dissertationsleiter)

Prof. Dr. Marlene Bartos

(Korreferent)

Basel, 21.02.2017

Prof. Dr. M. Spiess

(Dekan)

Contents

Abstract

During auditory fear conditioning, an animal learns to associate a neutral sound stimulus (CS) with an aversive foot shock (US). Processing of the CS in auditory cortex is altered during and after learning. In this thesis, the role of different subpopulations of neurons during and after fear conditioning is examined.

Auditory cortex responses during fear expression are investigated. A subpopulation of calretinin (CR)- positive interneurons and pyramidal cells show an increase in response size to the conditioned stimulus, suggesting the existence of a similar microcircuit in auditory cortex mediating salient sound information during fear expression. Vasoactive-intestinal polypeptide (VIP) – positive interneurons do not show such a CS-evoked increase in response size, hence CR-positive interneurons involved in fear expression are most likely VIP negative. Furthermore, discriminability between the CS and a neutral control sound is increased after fear learning.

Taken together, the data suggests the existence of a microcircuit involving CR-positive interneurons and pyramidal cells in auditory cortex which mediates behavioural saliency of sounds during memory expression.

Introduction

The brain enables humans and animals to gather information about their environment, and meaningfully interact with it. Sensory information, like the notes of a song, enters the central nervous system through sensory organs like the ears, is transformed into electrical signals and then sent to many different parts of the brain where it is received by highly interconnected neuronal circuits. These neuronal circuits integrate sensory information and send it to behavioural output stations, eventually leading to behavioural reactions like dancing, or emotional reactions, like happiness.

However, living and surviving in an ever changing environment requires the brain to be flexible, so that the organism can adapt to altered circumstances. The psychological term for these adaptions is learning, and these adaptations can be stored and recalled as memories. In animals, learning is typically accomplished through the association of a sensory cue with a particular consequence. The behavioural relevance of a stimulus is updated and the updated information is being integrated into a neuronal circuit that already drives numerous other behaviours (Mayford et al, 2012). During a memory test, the learned stimulus is presented, the updated information is recalled and an appropriate reaction is carried out.

These psychological phenomena are the behavioural evidence of changes occurring in neuronal circuits during learning, both on the molecular and the circuit level (Milner et al, 1998, Mayford et al, 2012). Over the last decades, a large array of studies over the last decades has been able to show that learning causes both short-term and long-term synaptic plasticity, which in turn leads to changes of the synapse on the molecular level (Goelet et al., 1986; Montarolo et al., 1986, Review: Fanselow & Poulos, 2005, Nabavi et al, 2014). These synaptic changes alter the response of a neuron to the learned cue when the organism is presented with it again during a memory test, without altering sensory responses to neutral stimuli. Evidence of plasticity has been found in many brain areas during learning, refuting the idea of a central memory core in the brain (McDonald et al, 2004, Squire, 2004, Weinberger, 2015). Instead, it would appear that memory

is a concerted effort of many brain areas, if not of the whole brain, including innumerable neurons organized in neuronal circuits.

The cortical circuit

One extensively studied neuronal circuit is located in the cortical mantle in the brain of rodents. The 'canonical' cortical circuit is found to be generally conserved between different sensory areas (Harris & Mrsic-Flogel, 2013, Harris & Shepherd, 2015). Excitatory drive from thalamus arrives directly into Layer 4 and Layer 2/3, although thalamic efferents also connect to layer2/3 through the distal dendrites in Layer 1. Layer 2/3 sends projections down to layer 5, and to other cortical areas (Harris & Mrsic-Flogel, 2013, Harris & Shepherd, 2014). The finding that neurons sharing an input source are also more likely to be connected (Yoshimura et al, 2005, Yassin et al, 2010, Harris & Mrsic-Flogel, 2013) lead to the conclusion that cortical Layer 2/3 is comprised of many highly interconnected subnetworks. The functional advantage of having recurrently connected subnetworks sharing common input lies in a higher signal-to-noise ratio even for short stimuli, and the ability to selectively boost behaviourally relevant stimuli represented by discrete subnetworks (Bathellier et al, 2012, Harris and Mrsic-Flogel, 2013).

GABAergic interneuron connectivity has been found to be much less specific with regards to forming functionally similar subnetworks like principal cells do, since the connection probability to a neighboring pyramidal cell is almost 100% for paralbumin (PV) - and somatostatin (SOM) - positive interneurons. Interneuron specificity seems to arise through their axonal target, both by targeting specific cell types and different subcellular compartments (Harris and Mrsic-Flogel, 2013).

Interneurons are commonly classified based on expression of a number of molecular markers (Petilla Interneuron Nomenclature Group, 2008, Fig. 1). These groups, while they are as close to representing a functional classification as we can come with current technology, are still quite diverse. 3 non-overlapping interneuron markers can be identified in sensory cortex: PV (40%), SOM (30%) and ionotropic serotonin receptor (5HT3aR) (30%) (Rudy et al, 2010, Tremblay et al,

2016). PV and SOM-interneurons both target pyramidal cells directly, albeit in different sub compartments, and are found throughout all cortical layers except Layer 1. 5HT3aR-positive neurons preferentially target other interneurons (Fig). The 5HT3aR population can be further subdivided into VIP- and non-VIP expressing cells, with the former being enriched in Layer 2/3 and the latter comprising most neurons in L1 (Tremblay et al, 2016).

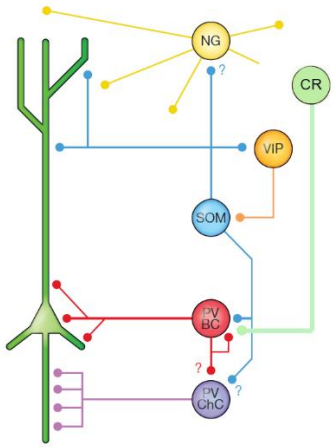

Figure 1: Canonical connectivity of different interneuron groups defined by expression of molecular markers. (Adapted from Harris and Mrsic-Flogel, 2013, to include CR-positive interneurons and connectivity proposed in Caputi et al, 2009)

Calretinin-positive interneurons

Compared to PV, SOM and even VIP, calretinin (CR) has been an understudied interneuron marker. Experiments carried out in somatosensory and visual cortex have found CR to be co-expressed with both SOM and VIP (Xu, 2010, Kawaguchi & Kubota, 1996). Whole-cell recordings of cortical CR-positive interneurons have shown that they are strongly connected amongst each other, as well as other interneurons (Caputi et al, 2009), and they are comprised of 2 different morphological subtypes, a bipolar subtype and a multipolar subtype (Caputi et al, 2009). This corresponds with findings that CR interneurons co-express other interneuron markers (Gonchar and Burkhalter 1999, Xu, 2010, Tremblay et al, 2016). Most CR interneurons are found in layer

2/3 and in lower layer 1 (Xu, 2010). Interestingly, CR interneurons have been shown to express nicotinic acetylcholine receptors (Porter et al, 1999). These findings put CR interneurons at the intersection between the cholinergic neuro-modulatory system known to signal behavioural relevance (see below) and sensory integration in the primary sensory cortices, making these interneurons a prime site of learning-mediated plasticity.

Layer 1 interneurons

Cortical layer 1 is unique in that it contains very few neurons, virtually all of which are GABAergic interneurons. Layer 1 receives input from cortical projections originating in lower layers of the same cortical column as well as long-distance excitatory drive from other cortical areas, in addition to thalamo-cortical and neuromodulatory afferents, making it a vital relay station for information entering the cortical column (Harris & Mrsic-Flogel, 2013). Layer 1 interneurons provide inhibitory input onto distal dendrites of pyramidal cells (Chu et al, 2003). In Layer 2/3, they have been shown to target both the somata of L2/3 pyramidal cells (Wozny and Williams, 2011), the apical dendrites of Layer 5 pyramidal cells (Jiang et al., 2013) and other interneurons (Jiang et al., 2013).

The auditory system

Perceiving sounds is a vital skill for an organism, as hearing enables predator detection as well as interspecies communication. In mammals, sound information enters the brain through the tympanum, travels through the middle ear and enters into the cochlea. The oscillation of the cochlear membrane moves hair cells attached to it, transforming frequency and amplitude information into electrical current which gets transmitted into the auditory brainstem (Hudspeth, 1989). From the auditory brainstem, sound information is forwarded through the midbrain to the auditory thalamus (MGm, MGv, Smith & Spirou, 2002), and from there distributed to auditory cortex (ACX), amygdala, and other brain areas (Smith & Spirou, 2002, Herry & Johansen, 2014).

Sound responses in auditory cortex have been extensively studied. Individual excitatory cells have long believed to be linear filters, ordered in sequence to encode sound characteristics. This however was found not to be true. Instead, responses of individual pyramidal cells to sounds depend heavily on the immediate 'sound history' of the neuron, i.e. other sounds preceding the current one (Chen et al, 2015, Kato et al, 2015, Christianson et al, 2011, Ulanovsky et al, 2004). Additionally, the current state of the animal influences ACX sound responses, i.e. quiescent, running, sleeping (Otazu et al, 2009, Zhou et al, 2014, Atiani et al, 2009), and learning-induced plastic changes alter sound-evoked response properties (Bathellier et al, 2012, Quirk et al, 2003, Bakin & Weinberger 1990). It is worth noting that not only frequency representation is altered by the factors mentioned, but also temporal characteristics of sound responses and sound level encoding can be affected (Bao et al., 2004; Polley et al., 2004). These plastic phenomena are discussed in detail in the following section.

Habituation to behaviourally neutral sounds

A critical function of the auditory system is to detect specific, behaviourally relevant sounds, whereas meaningless noise is ideally ignored. To this end, stimulus-specific adaptation is believed to decrease responsiveness to repeatedly presented tones that don't have any behavioural consequence (Chen et al, 2015, Ulanovsky et al, 2003). This habituation of the sound response has been observed on a minute-to-minute timescale (Chen et al, 2015), with response size decreasing after only a few presentations of the same tone. In addition, it can also be observed on a day-to-day basis (Kato et al, 2015), with excitatory cells exhibiting reduced responsiveness after several days of sound exposure. Interestingly, these findings where not limited to excitatory cells, but both PV- (Chen et al, 2015) and SOM-positive interneurons (Chen et al, 2015, Kato et al, 2015) were found to undergo similar plasticity. It is important to note that while Chen et al. found a general reduction of the excitation-inhibition balance in ACX during passive listening, their experiments were of a much shorter timescale (minutes-hours) than Kato et al.'s, who imaged the same cells over several days and only found effects in SOM-positive interneurons and

pyramidal cells. This suggests that short-term adaption might be governed by a different mechanism than habituation over several days.

Auditory cortex responses are state-dependent

Contrary to visual cortex, where active states such as running boost sensory responses, auditory cortex decreases its response size to sound stimuli during locomotion (Otazu et al, 2009, Zhou et al, 2014). Compared to a passive listening state, excitation-inhibition balance is reduced in ACX during animal motion, leading to reduced sound-evoked activity (Zhou et al, 2014). Interestingly, the active state does not only include locomotion, but also engaging in a learned auditory task (Otazu et al, 2009). However, Otazu et al. make the point that task engagement is different that selective attention to a specific sound, arguing that their task has a 'low attentional load', and propose that engagement suppresses auditory responses, so that attentional modulation might superimpose its effects. Generally, the biological advantage of decreasing ACX activation during active states remains elusive.

Learning-induced plasticity in auditory cortex

The only mechanism actually enhancing auditory responses in ACX found so far was plasticity related to learning an auditory task. (Weinberger 2015, Kato et al, 2015, Suga & Ma, 2003, Weinberger 2004, Quirk et al, 1997). Generally, these studies have shown that upon association of a tone with either reward or punishment, plastic changes in the receptive field of pyramidal cells are induced. Most studies using electrophysiological recordings identified a shift of the neuron's best frequency, i.e. the specific frequency generating the largest number of spikes, towards the target sound's frequency. This effectively increases the number of cells responding to the target sound, and the number of spikes generated, potentially improving detection of relevant sounds. It is worth noting that plastic changes caused by learning an auditory task are

usually found to be bidirectional, with neurons increasing as well as decreasing their responses to the target sound (Kato et al, 2015, Kuchibhotla et al, 2016).

Interneurons in auditory cortex are more broadly tuned than pyramidal cells, and hence contribute less to frequency tuning, but instead provide gain control and selective intensity tuning (Moore & Wehr, 2013). VIP-positive interneurons in auditory cortex have been shown to respond to reinforcement signals and mediate behavioural saliency through disinhibition of pyramidal cells (Pi et al, 2013). Recently, interneurons have also been implicated in signaling context switches in auditory cortex (Kuchibhotla et al, 2016). In general, the role of interneurons in auditory cortex during learning and memory is poorly understood.

The auditory cortex in fear conditioning

Probably one of the most often used paradigm to investigate learning- and memory-related plasticity in the auditory system is auditory conditioning. This behavioural paradigm was first made popular by Ivan Pavlov, who trained dogs to associate the ringing of a bell with food. Observing that the dogs would eventually start salivating at the ringing of the bell alone, he realized that pairing a neutral stimulus (the bell) with a salient stimulus (the food), the neutral stimulus would eventually acquire the same behavioural meaning as the unconditioned one, and provoke the same behavioural reaction, salivating. In auditory fear conditioning, a neutral sound called the conditonined stimulus (CS) is paired with a mild electrical foot shock (unconditioned stimulus, US), causing a rodent to exhibit a fear reaction in response to the CS presented alone after learning. This fear reaction is complete immobility of the body called freezing, and goes along with the fact that most rodent predators can only see moving targets, hence freezing is a great strategy to go undetected. In the laboratory, the length of a freezing episode is a good measure for the level of fear, and one that is easy to observe.

Research into neuronal circuits involved in the acquisition and expression of conditioned fear has shown that the amygdala, a brain structure located in the temporal lobes, is the ‘fear center’ of the brain (LeDoux, 2000, Maren, 2001). In its basolateral nucleus (BLA), neuronal activity caused

by both the foot shock and the sound converge (Fig. 2) (Romanski et al, 1993), and induce plasticity (Fig. 2; LeDoux, 2000, Herry & Johansen, 2014, Tovote et al, 2015).

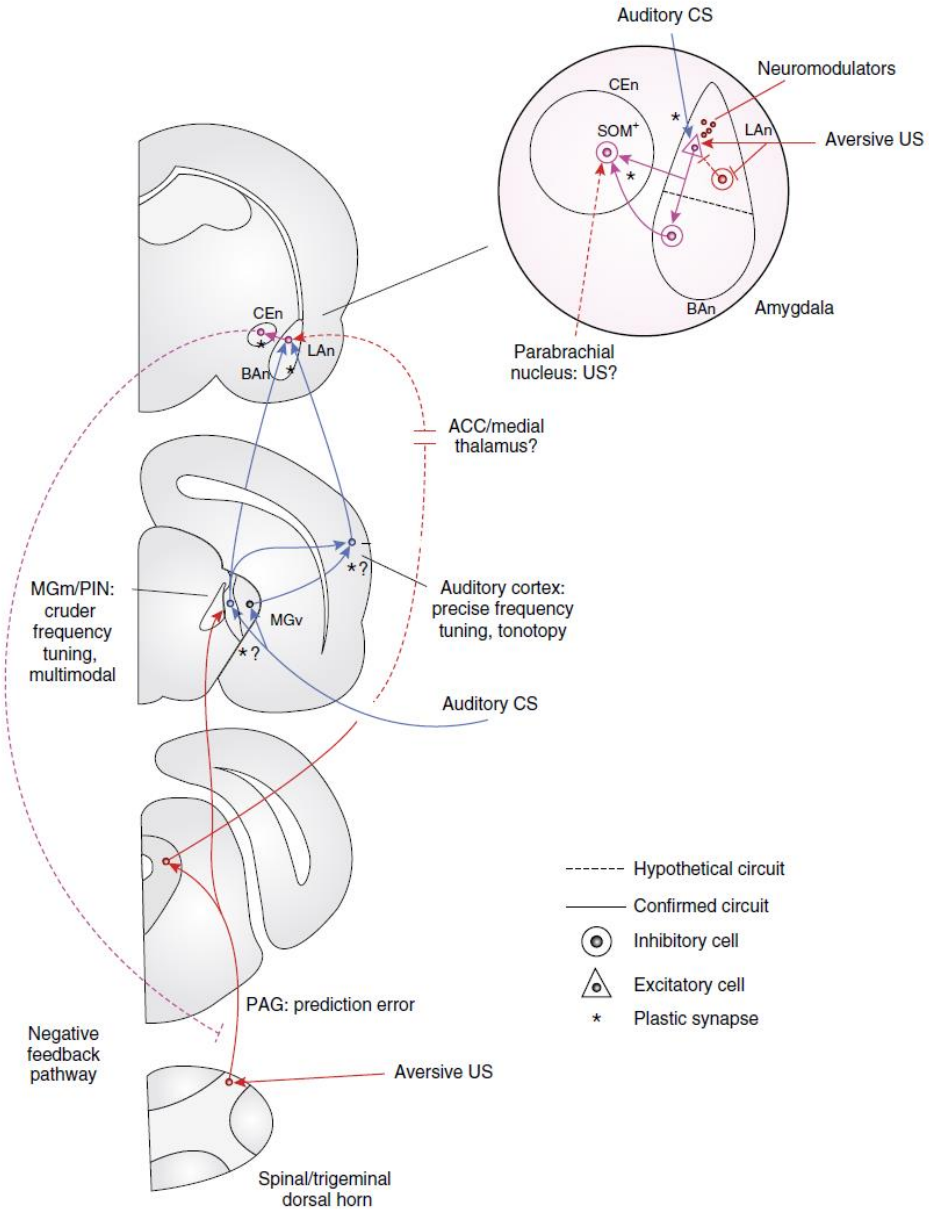

Figure 2: Neural circuits in auditory fear conditoning. (Adapted from Herry & Johansen, 2014)

Auditory sensory information arrives at the BLA from the thalamus, as well as from auditory cortex (Fig.2) (Romanski & LeDoux, 1993). Both auditory (MGm) and multisensory (MGv) thalamus are known to project there (Weinberger, 2004), and the latter even exhibits short-term plasticity during auditory fear conditioning (Weinberger, 2004, Antunes & Moita, 2010). As early as 1956, the first study showed plasticity in cat auditory cortex after fear conditoning (Galambos et al., 1956), being followed by electrophysiological studies confirming that single pyramidal cells in ACX change their firing patterns after associative learning (Diamond & Weinberger, 1984). Lesion studies showed that auditory cortex was not necessary for fear conditioning of simple pure tones in a non-discriminative protocol (DiCara et al, 1970, Teich et al, 1988, Romanski and LeDoux, 1992). However, for discriminative fear conditioning, auditory cortex is indeed required (Teich et al, 1988), and after lesioning auditory cortex, animals conditioned before the lesion did not undergo extinction (Teich et al, 1989), indicating a vital role for auditory cortex plasticity in acquisition and expression of conditioned fear.

Indeed, Layer 1 interneurons (see above) in ACX were found to be excited by the foot shock (Letzkus et al, 2011). This activation was mediated by cholinergic signaling from the nucleus basalis. In turn, layer 1 interneurons inhibit PV-positive interneurons in layer 2/3, which eventually release pyramidal cells from inhibition. This disinhibitory microcircuit underlies the observed increased sound-evoked activation of ACX pyramidal cells during fear conditioning.
The molecular identity of layer 1 interneurons involved in this microcircuit is not defined.

Neuromodulation mediates behavioural relevance to the cortical circuit

As mentioned above, a changing environment requires the brain to flexibly encode sensory information, which is achieved through plasticity of synapses. The cholinergic system in the basal forebrain has been shown to send saliency signals to the sensory cortices, in order to instruct the circuit on the behavioural relevance of a cue (Dekker et al, 1991, Richardson and DeLong, 1990). Acetylcholine is released diffusely into the cortex (Woolf, 1991) and binds to two types of receptors, nicotinic and muscarinic cholinergic receptors (Christophe et al, 2002). The effect of

acetylcholine is generally depolarizing across cell types (Poorthuis et al, 2014), with both pyramidal cells and all interneuron subtypes, with the exception of PV-positive interneurons, expressing cholinergic receptors (Kawaguchi, 1997, Gulledge et al. 2007), leading to a general increase in stimulus responsiveness (McKenna et al, 1988). Experiments of pairing basal forebrain stimulation with the presentation of a sound has produced learning-like increase in responsiveness of the affected auditory cortex cells, suggesting that cholinergic basal forebrain projections might indeed be responsible for learning-induced plasticity in auditory cortex (Hars et al, 1993, Dimyan and Weinberger, 1999).

Population analysis

Most of the results discussed above focused on single cell responses, and how they are affected by learning. However, single cells do not operate in a vacuum, but receive innumerable inputs and connect to countless downstream cells. This raises the question, whether the activity of a single cell is closely listened to by a downstream structure, or whether it is a population of cells whose coordinated activity contains the actual information (Pouget et al, 2003, Sanger, 2003).

Modern two-photon imaging techniques allow for simultaneous recordings of large populations of cells, while tracking the same individual cells over several days and closely observing their activity. Population data offers the possibility of more complex analysis methods, and the application of approaches born out of recent advances in information technology, like data mining from large datasets (Pouget et al, 2003, Quiroga & Panzeri, 2009, Sanger, 1996, Deneve et al, 1999, Latham & Roudi, 2010).

Many of those approaches base their analysis on simple statistical properties of the recorded activity of a population of cells, such as response size and duration. A common approach is to train a classifier to distinguish between neuronal signals which were evoked by different stimuli (Quiroga & Panzeri, 2009, Quiroga & Panzeri, 2013). If the classifier is successful in predicting which stimulus was presented based on neuronal data alone, it can be concluded that the neuronal population response elicited by the stimuli is different enough in its statistical

properties for an unbiased observer to correctly classify a novel stimulus. While this approach does not inform about whether a potential downstream source receiving this input is actually learning the same rules, it is a good approximation and nevertheless a useful tool to measure whether the recorded activity is potentially different enough to accomplish stimulus discrimination.

Aim

The aim of this thesis is to investigate the role of specific subpopulations of interneurons in the auditory cortex during fear acquisition and fear expression, and to elucidate the underlying circuit mechanisms.

This thesis will focus on the activity of CR- and VIP- positive interneurons during fear expression, as well as the dynamics of principal cells in auditory cortex. Computational data analysis will elucidate encoding power of the neuronal populations recorded.

Material and Methods

All experiments were performed in accordance with the guidelines of the Veterinary Department of the Canton Basel-Stadt, Switzerland.

Surgeries

6 – 8 weeks old male mice (for CR interneurons: CR-IRES-Cre, for VIP interneurons: VIP-IRES-Cre, for pyramidal cells: Cre-negative littermates) were deeply anesthetized with Isoflurane (3 - 5 % for induction, 1.5 % for maintenance, Attane, Piramal) and injected with Meloxicam i.p. (10 mg/kg, Metacam, Boehringer Ingelheim) and Ropivacaine s.c. (65 mg/kg, Naropin, Astra Zeneca). The right temporal muscle (m.temporalis) was gently loosened from the skull and fixed in place with histoacrylic (Braun) and superglue (Pattex). A 3 mm craniotomy was drilled over right ACX (center of craniotomy from bregma, anterior-posterior: -2.48 mm, lateral: +4.45 mm). 5-6 injections of either AAV2/1- DIO-ef1a-GCaMP6f (for interneurons, titer: 7.81e11 GC/ml) or AAV2/1- ef1a-GCaMP6f (for pyramidal cells, titer: 1.68e12 GC/ml) were made in the lateral ACX (depth: 500 um, injection volume: ~ 250 nl per injection) using borosilicate glass capillaries (World Precision Instruments) and a picospritzer (Föhr Medical Instruments GmbH). Subsequently, a 3 mm glass coverslip was fitted into the craniotomy and fixed with superglue (Pattex, Germany) and histoacryl (Braun, Country) to seal the skull tightly. The remaining skull surface was scratched using a hypodermic needle for better adhesion of the head bar, covered in histoacryl (Braun) for stabilization, and a custom made head bar was attached to the skull using dental acrylic (Paladur, Heraeus). During recovery, mice were group housed (2-4 animals/cage) in a fixed 12-hour day/night cycle and given continuous access to a running wheel, as well as to food and water ad libitum.

After 4 weeks of recovery and virus expression, the animals were anaesthetized using FMM (a mixture of Fentanyl (0.05 mg/kg; Actavis), Midazolam (5.0 mg/kg; Dormicum, Roche) and Medetomidine (0.5 mg/kg; Domitor, Orion) and the quality of the cranial window as well as the level of GCamp6f expression were assessed using a binocular (Leica). (The latter was only possible for pyramidal cells, as interneurons do not produce strong enough fluorescence for detection with small magnifications). If the window appeared clear with minimal scar tissue on the edges of the craniotomy, the animal was woken up (wake mix: Flumazenil (0.5 mg/kg, Anexate, Roche), Atipamezole (2.5 mg/kg, Antisedan, Pfizer)) and returned to the home cage to recover for at least 2 days.

Two-photon calcium imaging

For calcium imaging, the animal was placed under a custom-build two-photon microscope (Thorlabs) with a 12 kHz resonant scanner (Cambridge Technology). The angle of the objective was set to 49 degrees (vertical: 0 degrees) for all experiments. Calcium activity was visualized using a femtosecond laser (Insight, Spectra Physics) tuned to 930 nm, emission light was band-pass filtered using a 525/50 filter (Semrock) and recorded using a GaAsP photosensor (H7422, Hamamatsu). Signals recorded on the PMT were amplified (DHPCA-100, Femto), digitized (800 MHz, NI5772, National Instruments), and band-pass filtered (80 Mhz, digital Fourier-transform filter implemented in custom written software on an FPGA (NI5772, National Instruments)). A piezo-electric stepper allowed for 'simultaneous' acquisition of frames at 4 different imaging depths, reducing the actual scanning rate of 40 Hz to a 10Hz rate per imaging layer. The size of the acquired image was 400 x 750 pixels, translating to a 300 µm x 375 µm field of view.

Imaging setup

During imaging, the animal was head-fixed on its left side using a custom made head bar holder, providing access to the right auditory cortex. Animals were free to run on a spherical Styrofoam treadmill during the whole imaging experiment. Running activity was registered using a custom-

build infrared motion sensor pointed at the treadmill, and recorded using custom-written software (LabVIEW, National Instruments). 2 USB cameras (Microsoft), which had their UV filters removed, were pointed at both eyes and custom-written software (LabVIEW, National Instruments) was used to record pupil size. Pupil size is maximal in complete darkness, hence animals were provided with a virtual reality setting in the form of an endless tunnel whose movements were directly coupled to treadmill motion. This virtual reality provided baseline illumination, and therefore allowed for measurements of pupil dilation during the experiment. Reported pupil dilations are normalized by pre-condiitoning pupil dilations to account for large differences of absolute pupil size between individual animals.

All sound stimuli were presented through an electrostatic speaker (ES1, Tucker-Davis Technologies) facing the animal at about 30 cm distance. Both pure tones as well as frequency-modulated sweeps were generated using custom-written scripts in RPvdsEx (Tucker-Davis Technologies), digitized (RP2.1 processor, Tucker-Davis Technologies) and amplified using an ED1 speaker driver (Tucker-Davis Technologies). All sounds were adjusted to 75 dB, measured at the position of the animal.

For measuring the tuning of neurons, pure tone pips (4x 250 ms, 250 ms ISI) were used ranging from 3 kHz to 48 kHz, with a logarithmic increase in frequency between individual tones (13 different frequencies in total: 3, 4, 5, 6, 8, 12, 16, 20, 24, 28, 32, 40, 48, all in kHz); each frequency was presented 5 times in a random order. Time intervals between tone presentations were pseudo-randomly distributed with values ranging from 10s to 15s.

For fear conditioning, the stimuli used were up-sweep pips (10x 250 ms, 250 ms ISI, frequency-modulated sweep ranging from 5 – 15 kHz) and down-sweep pips (10x 250 ms, 250 ms ISI, frequency-modulated sweep ranging from 40 – 17 kHz); both conditioned stimuli were interchangeably used as CS+ and CS-. Tiem intervals between CS presentations were pseudo-randomly distributed between 90s to 120 s. The same auditory stimulation setup was used for both imaging experiments as well as freely-moving behaviour.

Fear conditioning

Fear conditioning was performed in a custom-build square Plexiglas context equipped with a shock grid (Small arena shock floor, Coulborn). Foot shock intensity was adjusted to 0.45 mA, and measured before each experiment. The speaker providing conditioned stimuli was mounted directly over the center of the context, and sound intensity was adjusted to 75 dB in the center of the context. During behavioural test, the animal was placed in a similar setup, with the square context being switched for a round Plexiglas context with a glass floor. Timestamps for both tone presentations and foot shocks were generated and subsequently recorded using custom-written scripts in AxoGraph X (Dr. John Clements) and digitized using an ITC-18 digitizer (HEKA Elektronik). The behaviour of the animal during fear conditioning and fear test was recorded using an USB camera (Microsoft) and Life Cam software (Microsoft). Videos were later replayed for analysis using Windows Media Player (Microsoft) and freezing was manually assessed. An episode of immobility was counted as freezing if the animal was stationary for at least 2 s at a time, and showed no evidence of grooming, or head movement.

The experiment started with mapping of the imaging site in auditory cortex using pure tones (see above). 24 hours later, the animal was presented with each CS four times (presented in random order) while calcium imaging of the auditory cortex was performed and baseline responses of neurons to the conditioned stimuli were acquired (Habituation).

For conditioning, the animal was placed in the conditioning context and was free to move around. During conditioning, the conditioned stimulus (CS+) was paired with a foot shock (1s duration). Every other trial, a neutral control tone (CS-) was presented which was not paired with a footshock. For unpaired control experiments, at least 90s passed between the CS+ and the foot shock. 24hrs after fear conditioning, the animal was subjected to a fear test in a different context (see above), during which the behavioural reaction to both CS- (presented 2 times) and CS+ (presented 2 times) was measured. After the fear test, the animal was returned to the home cage for 2 – 3 hours. Subsequently, the mouse was placed under the 2-Photon microscope and presented with 4 CS- which were followed by 4 presentations of the CS+ (Test).

Analysis of imaging data

Raw images were full frame registered using custom-written software in Matlab (Mathworks) to correct for any brain motion artifacts during running or grooming activity of the animal. Neurons were manually selected for calcium signal extraction based on the mean and maximum fluorescence projection; only neurons visible during the whole experiment (Tuning, fear conditioning) were selected. Slow drift of the raw fluorescent trace was corrected using an 8^{th}-percentile filtering with a 15s sliding window (Dombeck et al., 2007), and ΔF/F was calculated as the mean fluorescence of each selected neuron in each frame, subtracted and normalized by the median of the fluorescence distribution of the respective neuron. Further analysis was performed using custom-written functions in Igor Pro (Wavemetrics) and Matlab (Mathworks). Statistical tests were carried out in Matlab (Mathworks) and Prism (GraphPad). Wilcoxon test indicates Wilcoxon matched-pairs signed rank test for non-Gaussian distributed data. 2-tailed paired t-test was used for normally distributed data.

Principal component analysis and k-means clustering

Calcium activity during the CS+ before and after fear conditioning was averaged over all 4 trials per condition for each cell, and concatenated in a matrix.

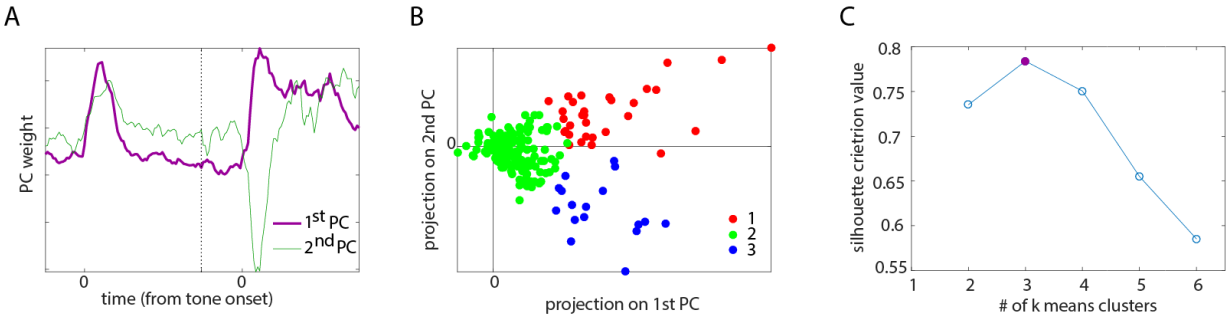

Figure 3: Illustration of clustering approach. A: Representative example of 2 principal components. Main source of variance is the sound response. First principal components selects sound-response cells (purple), second principal component selects differentially activated cells between both time points (green). **B:** K-means clustering based on 1^{st} and 2^{nd} principal component. Red dots: cluster 1. Green dots: cluster 2. Blue dots: cluster 3. **C:** Representative results of silhouette function run on 2-6 clusters. 3 clusters gives the highest average value, hence 3 clusters is the best fit for this particular dataset.

For dimensionality reduction, a principal component analysis was run on that matrix (Fig. 3A). For both the paired and the unpaired condition, principal component 1 and 2 together accounted for at least ~75% of the variability observed in the whole population. Principal component (PC) 1 selects for cells which are sound responsive, whereas PC 2 selects cells whose response is differentially modulated between both time points, that is, either an increase or a decrease in response size during Test. That leaves cells which never respond to either CS (and therefore also do not change their response after conditioning) close to 0 for both principal components.

To form functional groups based on the principal components, k-means clustering was performed to cluster similar cells together (Fig. 3B). Since k-means requires the experimenter to define the desired number of clusters, clustering has been repeated with the number of clusters ranging from 2 (minimum) up to 6 (as it would have been unlikely and probably meaningless to find more than 6 functional subgroups within all pyramidal cells in auditory cortex). For final determination of optimal number of clusters, the silhouette function was run on all clustering results. This function returns the 'cost' for each cell to be in the cluster it was assigned to, with well-fitting clusters returning high values, and ill-fitting low values. These values were averaged and the number of clusters yielding the highest silhouette value, and hence having most cells fit as well as possible, was chosen as the number of functional subgroups present in the population (Fig. 3C).

Thresholding

For quantification of significant trials, calcium data was binned (500 ms bins), and the mean (BL) and the standard deviation (STD) of each 5s baseline period preceding the sound presentation was calculated. The calcium trace during the sound presentation (RESP, 5s) was averaged, and the trial was counted as responsive, if the following condition was met:

$$RESP > BL + 3*STD$$

Population analysis: ROC analysis

For ROC analysis, the calcium data was binned (500ms bins) and the response size for each sound was calculated:

$$\text{Response} = \text{Mean (5s response)} - \text{Mean (5s baseline)}$$

The responses were sorted into bins such that each bin had on average 4 responses in it, and there were never more than 40 bins. These bins are plotted in histograms beneath each ROC curve (see Results).

2 classes of stimuli elicit different, noisy neuronal responses, whose distributions, when binned, might be more or less overlapping. The binary classifier employed during ROC analysis shifts the threshold ('criterion value' in the graph above) continuously along the x axis, assigning each value below it to one of the classes, and each value above it, to the other. As the threshold moves across the x axis, this simple classifier becomes more or less correct, depending on how much the distributions of the two classes overlap. The result of the classification is represented by plotting the false positive vs. the true positive classification incidents.

The ROC curve was calculated using Matlab's build-in ROC function based on the binned responses. The dotted 45 degree line represents the 'no-discrimination'-line, as it indicates an equal amount of true positives and false positives. Each point of the resulting ROC curve represents a sensitivity/specificity pair corresponding to a particular decision threshold.

Immunohistochemistry

After imaging experiments were completed, animals were deeply anaesthetized using Isoflurane (5 %, Attane, Piramal) and Avertin (custom-made, 336 mg/kg). After checking for paw reflexes and breathing rhythm, the animals were transcardially perfused using 15 ml of PBS followed by 50 ml paraformaldehyde (4% in PBS, pH adjusted to 7.3). Fixed brains were extracted and kept in 4% PFA at 4° for 2-3 hours, after which they were transferred to PBS and refrigerated.

For antibody staining and confirmation of the location of the injection sites, fixed brains were cut into 80 µm thick slices containing right auditory cortex (the left half of the slice was discarded to reduce antiserum volume during staining). Native fluorescence of GCamp6f was strong enough in all animals to not warrant a separate enhancer staining for visualization of expression.

After antibody staining, brain slices were mounted on gelatin-coated slides, dried, and coverslipped using Fluostab (custom-made anti-fade). Fluorescent cells were visualized on a laser-scanning confocal microscope (Axio Observer, LSM 710 scanning head, Carl Zeiss AG) using a multiline argon laser (488nm, green; 568 nm, red) and HeliumNeon laser (647, far-red). Images were gain- and offset- adjusted using a pixel saturation tool and subsequently recorded using Zen Black 2010 software (Zeiss). A 20x objective (Carl Zeiss AG) was used to produce tiles of confocal stacks (6 x 6), with each image being 1987 µm (1895 pixels) x 1987 µm (1895 pixels) x 27 µm (15 pixels) and containing all of the fluorescent cells in the respective slice. The location of the craniotomy was manually verified by producing maximum projections of the imaging sites and comparing the location to the mouse atlas (Paxinos, 2012); if the imaging site was not in auditory cortex, the animal was excluded from further analysis. For antibody quantifications, confocal stacks were loaded into Fiji (Schindelin et al., 2012) and their cell counter plug-in was used to manually quantify expression overlap.

Antibody staining protocol

3 x 15 mins 0.3% Triton in PBS (PBS-T) at room temperature

2 hrs 5% serum in PBS-T (10% serum in 3 mice) at room temperature

48 hrs 1:1000 primary antibody in 5% serum in PBS-T at 4°

3 x 10 mins PBS-T at room temperature

2 hrs 1:1000 secondary antibody in 5% serum in PBS-T at room temperature

3 x 15 mins PBS at room temperature

Antibodies and Reagents:

Primary antibodies for VIP and SOM staining:

Rat anti-SOM (Millipore, MAB354)

Rabbit anti-VIP (Immunostar, 20077)

Secondary antibodies for VIP and SOM staining:

Goat anti-rabbit 647 (Invitrogen, A21245)

Goat anti-rat 568 (Invitrogen, A11077)

Serum for VIP and SOM staining:

Normal goat serum (Millipore, S26-100ml)

Further reagents used:

Triton-X 100 (T) (Sigma-Aldrich, T8787 SIGMA)

Phosphate-buffered saline (PBS) (137 mM, custom-made)

Results

Assessing fear in head-fixed mice

Freezing, meaning complete immobility, is a behaviour widely used as a measure for fear level in mice (see above). After discriminative fear conditioning, the animal will exhibit freezing behaviour in response to the CS+ (Fig. 5A), whereas freezing will be low in response to the CS- . In an unpaired control group, this specific freezing response is notably absent, with the animal showing barely any fear reaction to either of the CSs (Fig. 5B).

Since freezing is defined by the absence of movement, a certain baseline level of animal motion is required between CS presentations, which is generally given by natural explorative behaviour of mice in a freely moving environment. During head fixation however, even when given the choice to run freely on a treadmill, mice cannot display explorative behaviour, hence baseline motion is lower and much more erratic, making it virtually impossible to quantify immobility as a measure of fear.

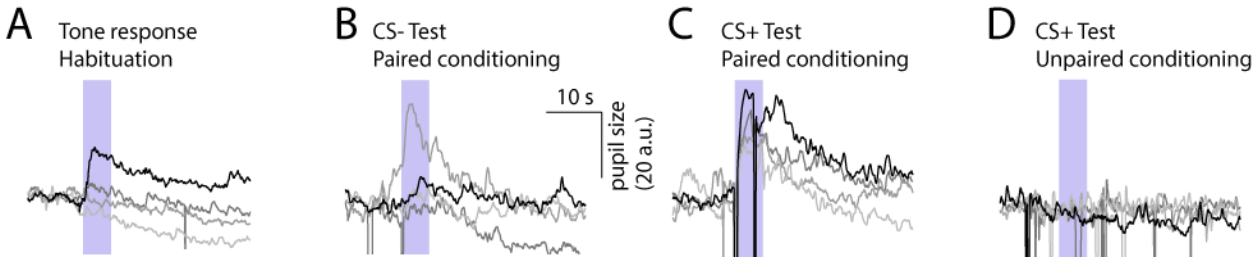

Figure 4: Evoked pupil responses. A: Pupil response to sounds in a naïve animal. First trial: black trace. Dark grey: second trial. Middle grey: third trial. Light grey: fourth trial. **B:** Pupil responses to CS- after fear conditoning. Colours: see A. **C:** Pupil responses to CS+ after fear conditoning. Colours: see A. **D:** Pupil response to CS after unpaired conditioning. Colours: see A.

A different measure easily accessible during head fixation is the size of the pupil. Previous studies (Lennartz & Weinberger, 1992) have implicated pupil size to be correlated with fear levels, with the diameter of the pupil increasing upon presentation of fearful stimuli.

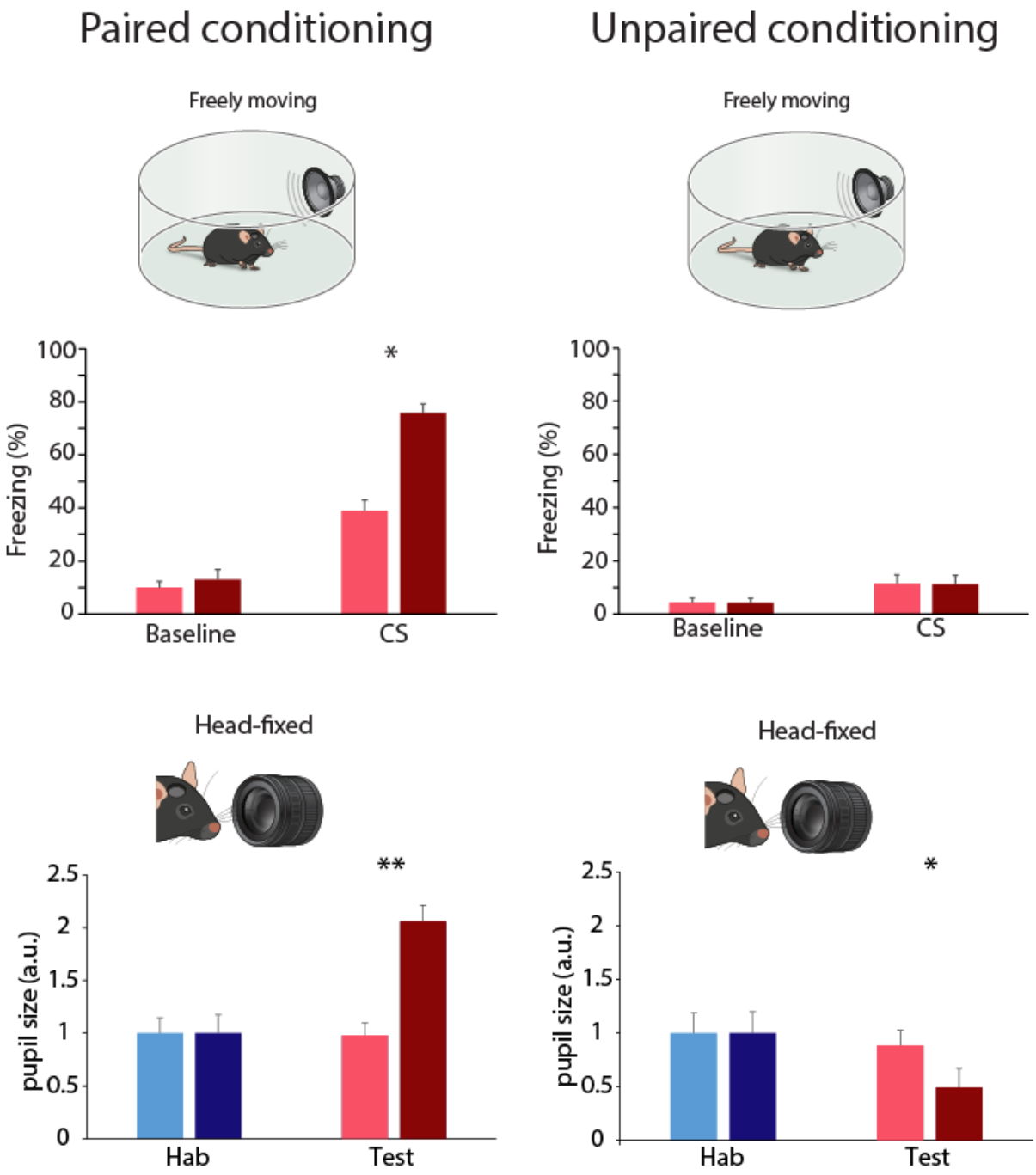

Figure 5: Measuring fear in freely moving and head-fixed mice. A: Mice exhibit specific increase in freezing in response to the CS+ compared to the CS-, but no fear in response to the context (baseline) (two-tailed t-test, $p<0.05$). **B:** In the unpaired group, mice do not show any freezing in response to the CS+. **C:** The size of the pupil is increased significantly in response to the CS+, but not the CS-. (Two-tailed t-test, $p = 0.0025$). Pupil sizes are normalized to the habituation size. **D:** In the unpaired group, the pupil size is significantly decreased in response to the CS+ compared to the CS-, as the animal habituates to sound exposure. (Two-tailed t-test, $p > 0.1$)

We took advantage of fact that the laser light used to image calcium activity illuminated the pupil and created a large contrast between the pupil and the iris. Indeed, when quantifying pupil size specifically in response to the CS+, we found a significant increase in its diameter compared to the CS- (Fig. 4A, C, Fig. 5C) (CS-: 0.97 ± 0.12, CS+: 2.06 ± 0.15, 2-tailed t-test: p = 0.0025). Again, similar to the freezing response, this difference is absent in unpaired control conditioned animals, where pupil size in response to CSs is very similar between both Habituation and Test, and CS+ and CS- after conditioning (Fig. 4D, Fig. 5D) (CS- : 0.88 ± 0.14, CS+: 0.49 ± 0.18, 2-tailed t-test: 0.10). Importantly, only pupil responses time-locked to the sound stimulus were analyzed. Taken together, these results suggest that pupil size is a good proxy for measuring fear levels in head-fixed mice.

Pyramidal cells in ACX are differentially modulated during fear expression

To measure potential plasticity in auditory cortex following fear conditioning, pyramidal cells in layer 2/3 of the auditory cortex were imaged before and after fear conditioning. To measure tuning, (see Methods), and to ensure that the imaging site was indeed in auditory cortex, animals were exposed to pure tones. Most pyramidal cells imaged in this study showed sharp tuning to frequency area (Fig. 6B). On the following day, the animal was exposed to both CS for the first time (see Methods), and a baseline response to both CSs' was acquired (Fig 6C, Fig. 6D, blue trace) (CS-: 5.53 ± 1.34 % ΔF/F, CS+: 6.86 ± 1.26% ΔF/F). For all animals, during habituation, layer 2/3 pyramidal cells showed sparse coding of the auditory stimulus, with only a few cells being responsive to the CS (Fig. 6C). After fear conditioning, pyramidal cells increased their response to the CS+ on average, while the average population response to the CS- was decreased (Fig. 6D, red trace) (CS-: 2.98 ± 1.28 % ΔF/F, CS+: 7.58 ± 1.24 % ΔF/F). In the unpaired control group (see Methods), the average response to both CS+ and CS- was slightly decreased (Fig 6C,D) (Habituation: CS-: 7.58 ± 0.78 % ΔF/F; CS+: 3.01 ± 0.5 %ΔF/F, Test: CS-: 6.89 ± 0.97 % ΔF/F, CS+: 2.78 ± 0.75 % ΔF/F).

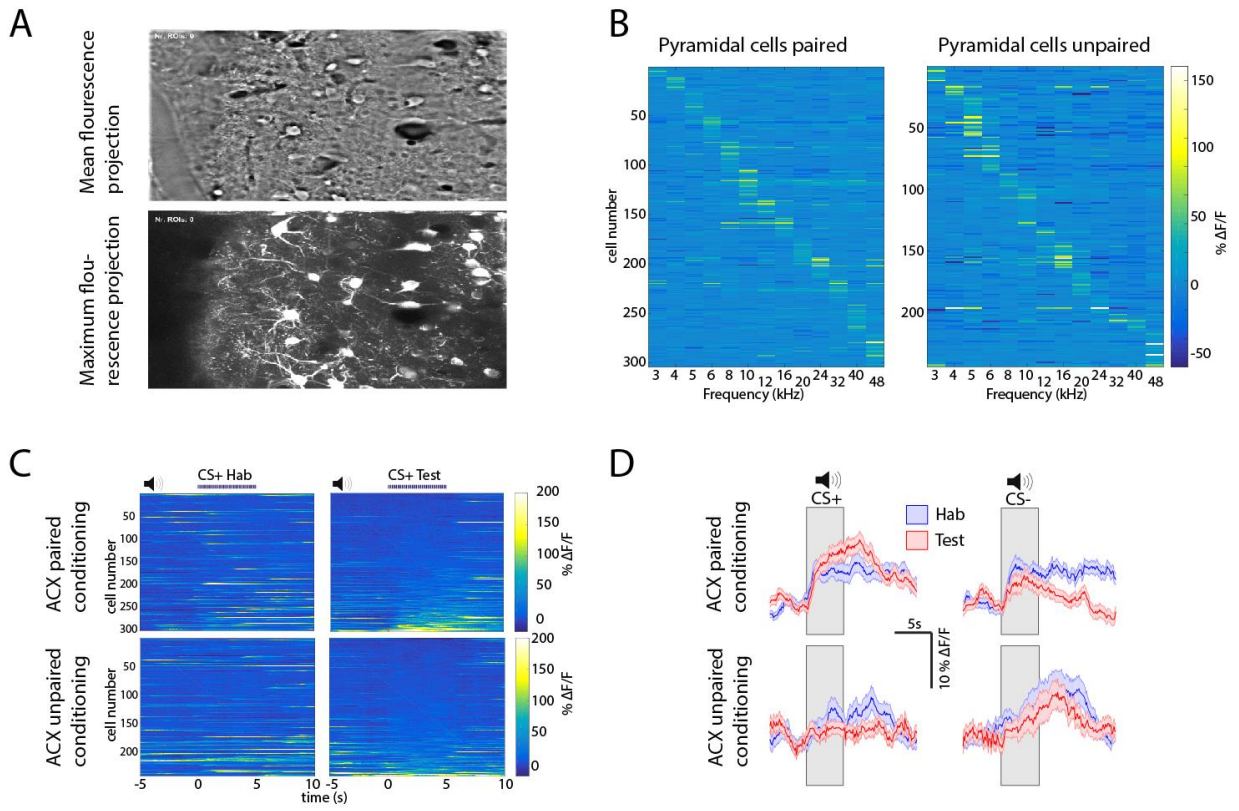

Figure 6: Sound responses of pyramidal cells in ACX. A: example pictures of pyramidal cells expressing GCamp6f in ACX. Top: mean fluorescence projection. Bottom: maximum fluorescence projections. Field of view: 300 µm x 375 µm**. B:** Pyramidal cells a narrowly tuned. Tuning curves are similar between animals in the paired and the unpaired group. **C:** Heat maps for all pyramidal cells. Each line is the average of 4 trials. **D:** Evoked responses of all pyramidal cells to CS+ and CS-. Error bars: SEM.

Individual cells' responses vary very widely from each other, hence the population average might not reflect changes in CS responses of individual cell groups very well. Therefore, we sought to functionally group those cells in an unsupervised manner, based on the change in response strength to the CS+ after learning (see Methods).

Pyramidal cells form 3 functional subgroups after fear conditioning. The largest group (n = 257) contains cells that are largely unresponsive to either CS (Fig. 7A, top panel) (CS+ Habituation: 2.26 ± 0.07% ΔF/F, Test: 2.82 ± 0.07% ΔF/F, CS- Habituation: 1.69 ± 0.08% ΔF/F, Test: 2.76 ± 0.13% ΔF/F). The second cluster (n = 21) contains cells responding very strongly to both CS+ and CS- before fear conditioning, but decrease their response strongly after (Fig. 7A, middle panel)(CS+

Habituation: 54.57 ± 10.60 % ΔF/F, Test: 4.16 ± 4.67% ΔF/F. CS- Habituation: 39.19 ± 10.97% ΔF/F, Test: -8.16 ± 7.28% ΔF/F). The third group (n = 26) responded modestly to both CS+ and CS- before conditioning, and shows a large, very specific increase in response size to CS+, but not the CS- (Fig. 7A, bottom panel)(CS+ Habituation: 13.81 ± 3.78% ΔF/F, Test: 57.34 ± 6.88% ΔF/F, CS- Habituation: 20.94 ± 7.29% ΔF/F, Test: 14.49 ± 6.04% ΔF/F).

In order to determine whether the responses of neurons became more or less reliable after fear conditioning, individual trials were classified into responsive or unresponsive (see Methods). As expected, cells which decrease their response to the CS+ after fear conditioning also had a decreased number of responsive trials to the CS+ after fear conditioning (Fig. 7C, Habituation: 1.67 ± 0.27 trials, Test: 1.05 ± 0.18 trials, Wilcoxon test: p = 0.093.). On the other hand, cells increasing their average response to the CS+ also significantly increased their response reliability (Fig. 7C) (Habituation: 1.15 ± 0.18 trials, Test: 2.00 ± 0.23 trials, Wilcoxon test: p = 0.008). In addition, Cluster 1 increases the number of trials on average by a small percentage (Fig. 7C) (Habituation: 0.47 ± 0.05 trials; Test: 0.64 ± 0.05 trials, Wilcoxon test: p = 0.013). With the exception cluster 1, no group increased their number of responsive trials to the CS- (Fig. 7C) (Cluster 1: Habituation: 0.46 ± 0.05 trials, Test: 0.52 ± 0.05 trials. Wilcoxon test: p = 0.36. Cluster 2: Habituation: 1.76 ± 0.27 trials, Test: 0.76 ± 0.17 trials. Wilcoxon test: p = 0.004. Cluster 3: Habituation: 1.35 ± 0.25 trials, Test: 0.96 ± 0.18 trials. Wilcoxon test: p = 0.20.)

Additionally, this figure illustrates the sparseness of neural responses in cortical layer 2/3. On average before conditioning, the most responsive cells (Cluster 2) respond to less than 2 trials out 4, while the majority of cells (Cluster 1) only responds to about 0.5 trials out of 4.

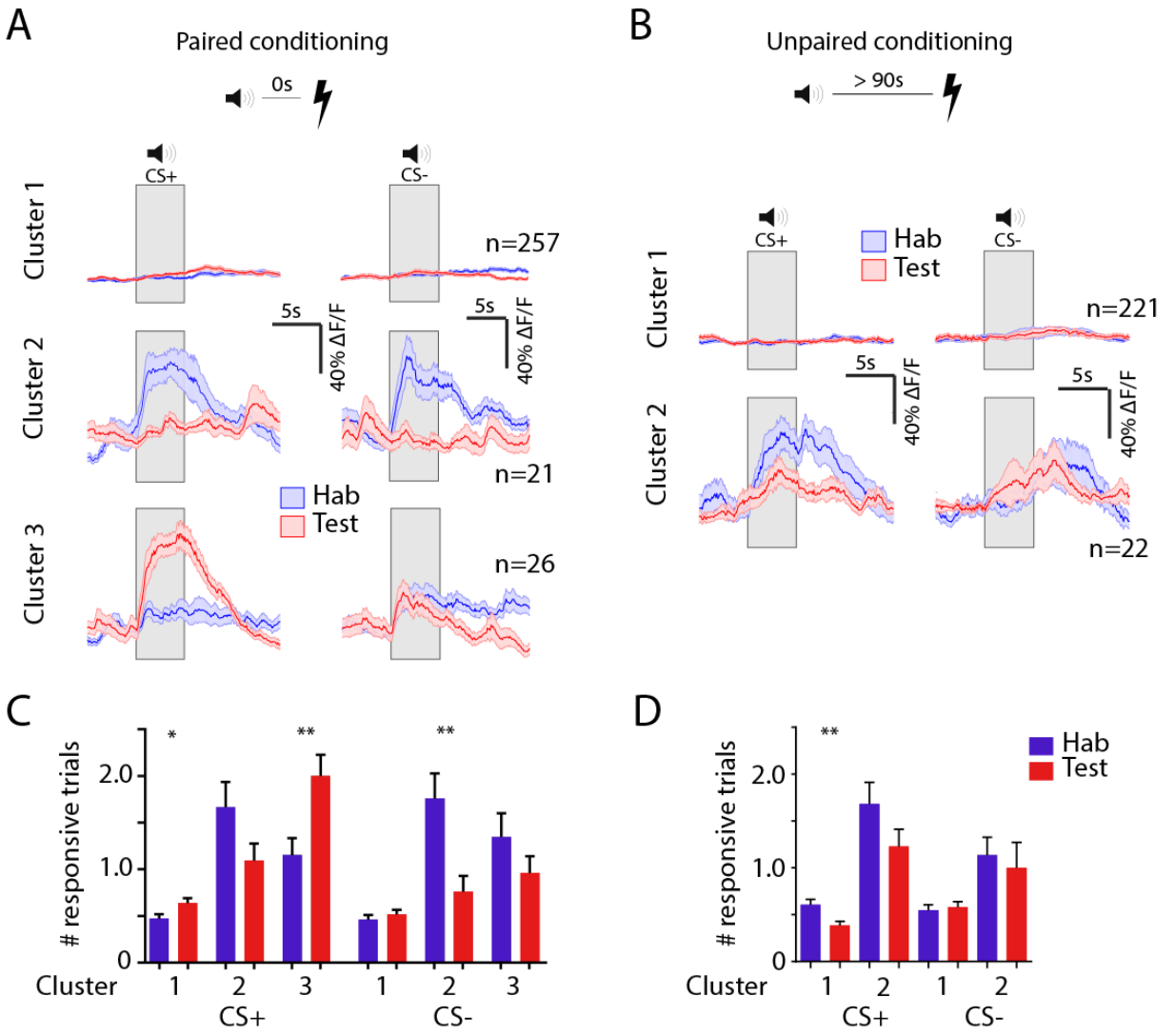

Figure 7: Functional subgroups of pyramidal cells in auditory cortex. A: Pyramidal cells of fear conditioned animals form 3 functional subgroups. **B:** In animals going through the unpaired paradigm, pyramidal cells form 2 functional subgroups. **C:** Number of responsive trials for paired pyramidal cell responses. **D:** Number of responsive trials for unpaired pyramidal cell responses. All error bars: SEM.

In animals undergoing unpaired conditioning, no increase in the CS+-evoked response during Test was observed (Fig. 6D) (CS+ Habituation: 3.25 ± 1.65% ΔF/F, Test: 0.96 ± 1.17% ΔF/F, CS- Habituation: 4.06 ± 2.31% ΔF/F, Test: 2.64 ± 2.11% ΔF/F). Concomitantly, only 2 functional subgroups could be found (Fig. 7B). The largest group (n = 221) was comprised of unresponsive cells (CS+ Habituation: 0 ± 0.09% ΔF/F, Test: 0 ± 0.10% ΔF/F, CS- Habituation: 3.49 ± 2.47% ΔF/F, Test: 1.32 ± 2.05% ΔF/F), while the second group (n = 22) contained cells which responded

strongly to the CS+ before conditioning, and decreased their responses during fear expression (Fig.7B, bottom panel). Responses to CS- are unaltered (Fig. 3E, right panel) (CS+ Habituation: 40.41 ± 13.13% ΔF/F, Test: 23.77 ± 5.81% ΔF/F, CS- Habituation: 9.85 ± 6.18% ΔF/F, Test: 15.83 ± 10.68% ΔF/F).

Looking at the reliability of the evoked responses, all cells decrease their number of responsive trials during fear expression (Fig. 7D) (CS+: cluster 1: Habituation: 0.61 ± 0.06 trials, Test: 0.38 ± 0.04 trials. Wilcoxon test: p = 0.001. Cluster 2: Habituation: 1.68 ± 0.23 trials, Test: 1.23 ± 0.19 trials. Wilcoxon test: 0.12. CS-: Cluster 2: Habituation: 1.14 ± 0.19 trials, Test: 1.00 ± 0.27 trials, Wilcoxon test: 0.12), with the exception of Cluster 1 in response to CS-, which stays constant (Habituation: 0.55 ± 0.06 trials, Test: 0.58 ± 0.06 trials, Wilcoxon test: p =0.72).

Taken together, this suggests that a subset of pyramidal cells specifically increased their response to the CS+ during fear expression. In addition, their response became more reliable. Pyramidal cells decreasing their response to the CS+ could be found in conditioned animals as well as in the unpaired control group; in both groups, these cells responded to a decreased number of sound presentations.

CR-positive interneurons form differentially modulated subpopulations during fear expression

CR-positive interneurons located in layer 2/3 were imaged before fear conditioning and during fear expression. Similarly to pyramidal neurons, tuning was also tested in those interneurons (Fig. 8B). In contrast to the sharp tuning of the pyramidal cells, CR interneurons appeared to be widely tuned.

Imaging CS responses during fear expression yielded a similar results as it did for pyramidal cells. The response to the CS+ was slightly increased after conditioning (Fig. 8C, D) (CS+ Habituation: 13.99%, CS+ Test: 16.67%), while the response to the CS- was decreased (Fig. 8D) (CS- Habituation: 16.76 ± 1.76%, Test: 10.3 ± 1.25%). In the unpaired control group, both responses

to CS+ and CS- were strongly reduced after conditioning (Fig. 8C, D) (CS+ Habituation: 34.77 ± 3.52% ΔF/F, Test: 8.5 ± 1.50% ΔF/F. CS- Habituation: 17.69 ± 2.16% ΔF/F, Test: 9.45 ± 1.65% ΔF/F).

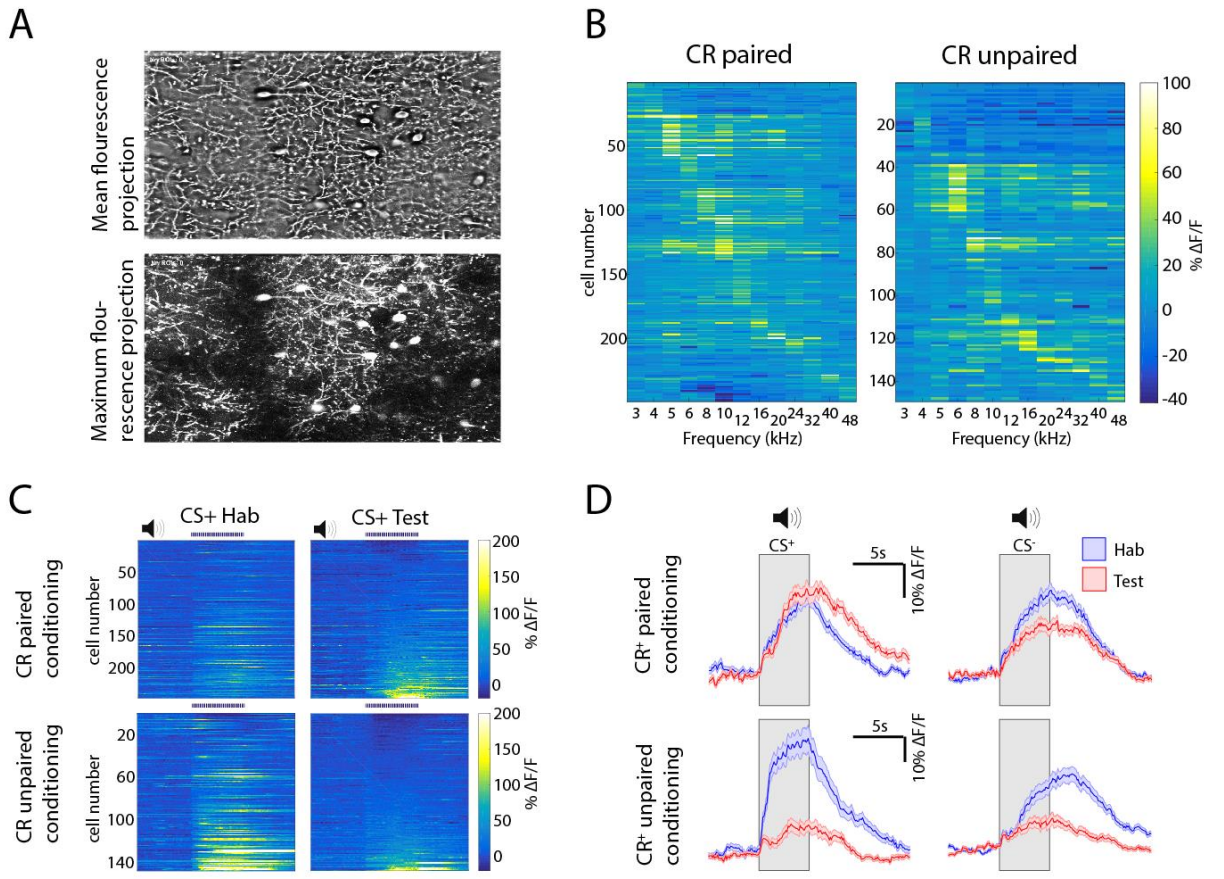

Figure 8: Sound responses of CR-positive interneurons. A: Example pictures of Cr-positive interneurons in ACX. Top: mean fluorescence projection. Bottom: maximum fluorescence projections. **B:** CR-positive interneurons are widely tuned. Tuning curves are similar between animals in the paired and the unpaired group. **C:** Heat maps of sound responses for all CR-positive interneurons. Each line is the average of 4 trials. **D:** Evoked responses of all CR-positive interneurons to CS+ and CS-.

Again, diversity in activity observed in the whole population of CR-positive interneurons was poorly reflected in the population average, so the same clustering approach (see above) was implemented to form functional groups of CR interneurons. For the paired group, 3 clusters could be identified: the first and largest cluster (n = 156) contained cells mostly non-responsive to either CS, before or after fear conditioning (Fig. 9A, top panel) (CS+ Habituation: 4.43 ± 4.00%

ΔF/F, Test: 5.59 ± 1.89% ΔF/F, CS-: Habituation: 8.19 ± 3.75% ΔF/F, Test: 5.03 ± 2.41% ΔF/F). The second cluster (n = 52) contained cells strongly responsive to both CS before conditioning, but decreasing their response size after (Fig. 9A, middle panel) (CS+ Habituation: 32.69 ± 4.00% ΔF/F, Test: 18.01 ± 1.89% ΔF/F, CS- Habituation: 32.32 ±3.75% ΔF/F, Test: 8.26 ±2.41% ΔF/F). The last group (n = 41) was comprised of cells modestly responsive to both CS during habituation, but strongly increasing their response to the CS+ during fear expression (Fig. 9A, bottom panel) (CS+ Habituation: 26.65 ± 0.07% ΔF/F, Test: 57.11 ± 0.1% ΔF/F). Response size to the CS- stayed constant (CS- Habituation: 29.63 ± 0.09% ΔF/F, Test: 32.94 ± 0.09% ΔF/F).

Looking at the reliability of the responses, similar changes were observed for CR-positive interneurons compared to pyramidal neurons. Cells in cluster 2 decreased their evoked CS+ response; these cells significantly decreased the number of responsive trials after conditioning (Fig. 9C) (Habituation: 2.73 ± 0.19 trials, Test: 1.72 ± 0.14 trials, Wilcoxon test: $p = 0.0007$). CR-positive interneurons in cluster 3 significantly increased the number of trials they responded to (Fig. 9C) (Habituation: 2.02 ± 0.23 trials, Test: 2.83 ± 0.13 trials, Wilcoxon test: $p = 0.004$). All functional subgroups of CR-positive interneurons decreased the number of responsive trials to the CS- (Cluster 1: Habituation: 1.26 ± 0.09 trials, Test: 0.81 ± 0.08 trials, Wilcoxon: $p<0.0001$. Cluster 2: 2.48 ± 0.19 trials, Test: 1.10 ± 0.17 trials, Wilcoxon: $p<0.0001$. Cluster 3: Habituation: 1.97 ± 0.20 trials, Test: 1.83 ± 0.19 trials. Wilcoxon test: $p = 0.6$). Overall, trial-to-trial variability was smaller for CR+ interneurons compared to pyramidal cells. CR-positive interneurons who responded to either CS before conditioning (largely cells in Cluster 2) responded to almost 3 trials out of 4 (Fig. 9C).

In the unpaired group, only the first 2 clusters could be observed. The largest cluster contained cells modestly responsive to CS+ during Habituation. These neurons lost their response completely over the course of the experiment (Fig. 9B, top panel) (CS+ Habituation: 16.99 ± 1.89% ΔF/F, Test: 2.73 ± 1.00% ΔF/F, CS- Habituation: 13.42 ± 1.88% ΔF/F, Test: 7.88 ± 1.54% ΔF/F). The second cluster included cells strongly responsive to both CS before, but very modestly responsive to CS after conditioning (Fig. 9B, bottom panel) (CS+ Habituation: 102.43 ± 6.89% ΔF/F, Test: 30.48 ± 4.29% ΔF/F. CS- Habituation: 33.94 ± 6.90% ΔF/F, Test: 15.44 ± 5.31% ΔF/F).

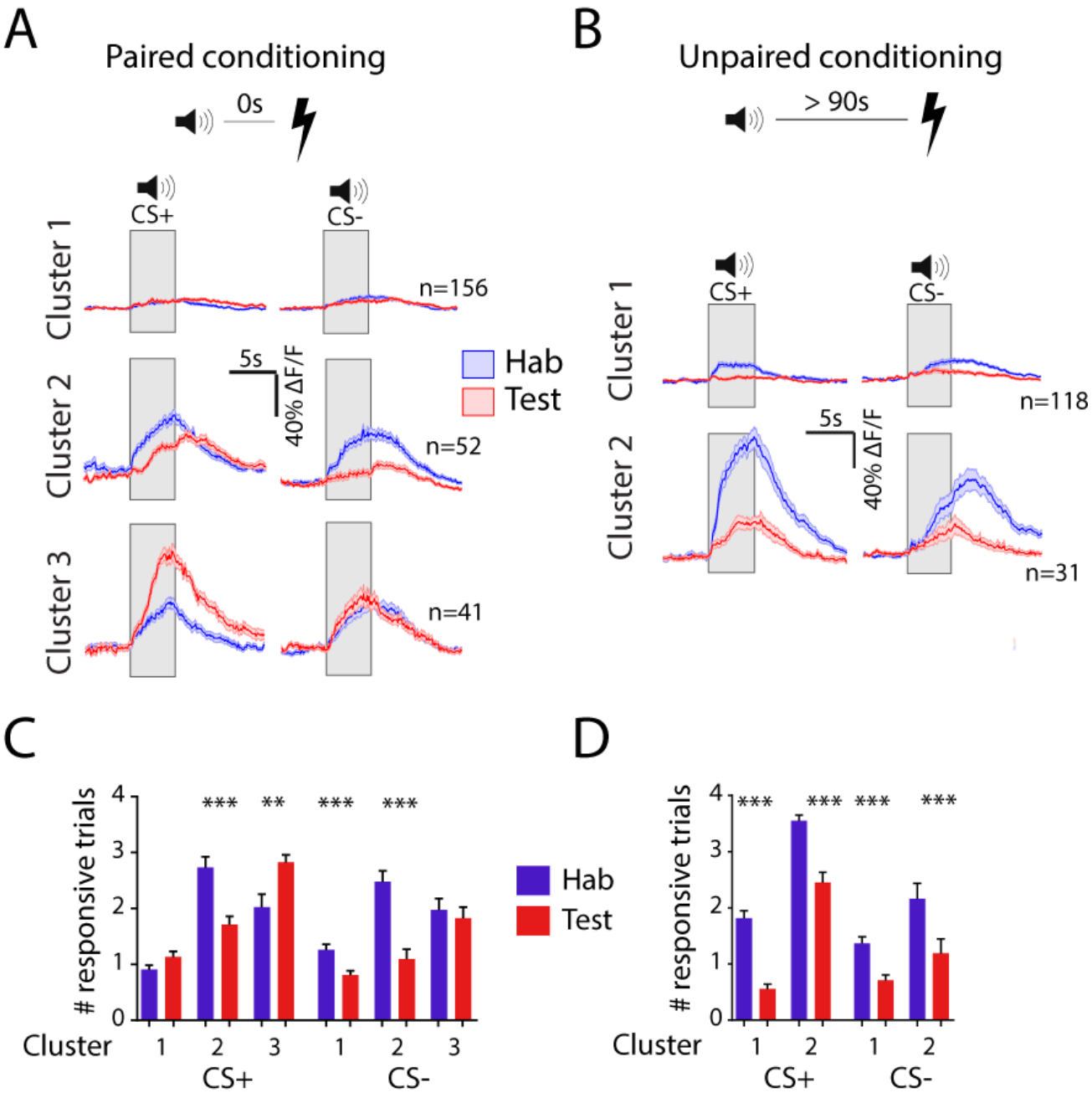

Figure 9: Functional subgroups of CR-positive interneurons in ACX. A: CR-positive interneurons of fear conditioned animals form 3 functional subgroups. **B:** In animals going through the unpaired paradigm, CR-positive interneurons form 2 functional subgroups. **C:** Number of responsive trials for paired CR-positive interneuron responses. **D:** Number of responsive trials for unpaired CR-positive interneuron responses.

Similarly to pyramidal cells, the number of responsive trials decreased after tone and foot shock exposure, with all cell groups decreasing their number of responsive trials over the course of the experiment (Fig. 9D). (CS+: Cluster 1: Habituation: 1.81 ± 0.14 trials, Test: 0.56 ± 0.08 trials, Wilcoxon test: $p<0.0001$. Cluster 2: Habituation: 3.55 ± 0.10 trials, Test: 2.45 ± 0.18 trials, Wilcoxon test: $p<0.0001$. CS-: Cluster 1: Habituation: 1.36 ± 0.12 trials, Test: 0.71 ± 0.09 trials, Wilxocon: $p<0.0001$. Cluster 2: Habituation: 2.61 ± 0.28 trials, Test: 1.19 ± 0.25 trials, Wilcoxon: $p = 0.0006$).

Taken together, these results strongly mimic the ones found for pyramidal cells, leading to similar implications regarding the meaning of the observed changes in response size. Cells strongly decreasing their responses to the CS+ in both the paired and the unpaired condition could imply that those cells respond to novel stimuli and, with an increase in familiarity of the sound, decrease their response to it. CR interneurons increasing their response to the CS+ could only be found in fear conditioning animals, but not in the unpaired control group, implying that those cells might actually signal behavioural relevance of the CS+ to downstream targets.

Co-expression of VIP and SOM in CR-positive interneurons in ACX

As previously mentioned (see Introduction), CR-positive interneurons have been shown to co-express other interneuron markers, namely SOM and VIP. However, these data stem from immunohistochemistry experiments which have been carried in visual and somatosensory cortex (Xu et al, 2010).

To assess overlap of VIP and SOM with the CR interneurons imaged in this study, brain slices of CR-IRES-CRE animals expressing Cre-specific GCamp6f have been stained with antibodies against those two markers. 4.4% of CR interneurons imaged co-expressed SOM, while 31.4% co-express VIP, and surprisingly, 64.2% of interneurons expressed only CR (Fi. 10A).

The low number of SOM co-expressing CR-positive interneurons does not stem from the staining not working properly, as plenty of SOM-positive interneurons were found in ACX (Fig. 10B), but only 3% co-expressed CR.

Out of all VIP-positive interneurons, 39.3% co-expressed CR (Fig. 10C). Since several functionally different subgroups of CR-positive interneurons were found (see above), co-expression of VIP might define one of these functional subgroups on a molecular level.

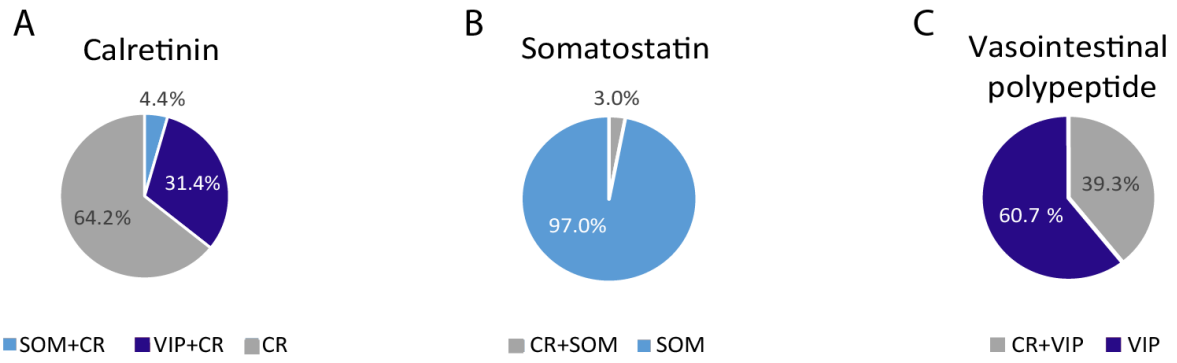

Figure 10: Overlap of CR-interneurons with other interneuron markers. A: CR-interneurons expressing CGamp6f co-express VIP. **B:** Overlap between SOM-positive interneurons and CR-positive interneurons expressing GCamp6f. **C:** Overlap between VIP-positive interneurons and CR-positive interneurons expressing GCamp6f.

VIP interneurons do not show CS+-specific increase of evoked responses during fear expression

To answer this question, VIP interneurons were imaged before and after fear conditioning. Similarly to CR interneurons, VIP interneurons were broadly tuned (Fig. 11A). As a population, they show a small response to CS before conditioning (Fig. 11B, C), and the response size is decreased after conditioning for both CS (CS+ Habituation: 13.22 ± 1.50% ΔF/F, Test: 6.20 ± 1.15% ΔF/F, CS- Habituation: 19.09 ± 1.75% ΔF/F, Test: 9.39 ± 1.25% ΔF/F).

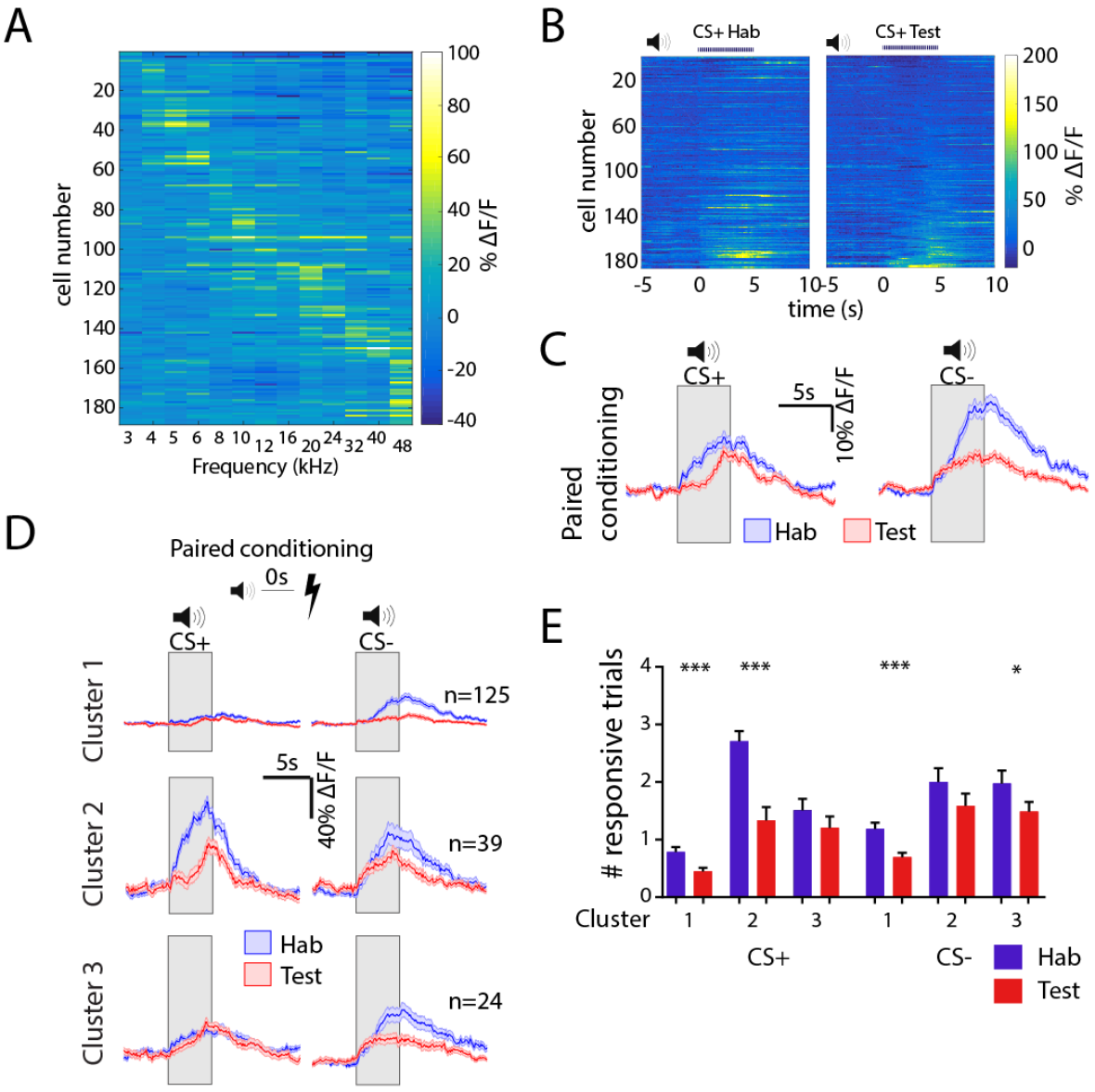

Figure 11: Sound responses of VIP interneurons. A: Tuning of VIP interneurons in naïve animals. **B:** Heat map of VIP-positive interneurons' response to the CS+. Each line is an average of four trials. **C:** Population average of CS+ and CS- responses of VIP interneurons. **D:** Functional subgroups of VIP-positive interneurons. Analysis as described in the methods returned 2 functional subgroups (Cluster 1 & 2). Even when separating the dataset into 3 clusters, there is no subpopulation increasing their responses. **E:** Number of responsive trials for VIP-positive interneurons in fear conditioned animals.

Clustering of the data revealed 2 functional subgroups of VIP interneurons. Cluster 1 contained the largest number of cells (n = 125) (Fig. 11 D, top panel), which are largely unresponsive to the

CS+, but show a modest response to CS- (CS+ Habituation: 3.93 ± 0.77% ΔF/F, Test: 1.33 ± 0.75% ΔF/F. CS- Habituation: 11.89 ± 1.51% ΔF/F, Test: 4.21 ± 0.89% ΔF/F). This response disappeared after conditioning. Cluster 2 contained cells strongly responding to both CS before the conditioning, but during fear expression, responses were strongly diminished and, in the case of the CS+, also delayed (Fig. 11D, middle panel)(CS+ Habituation: 16.10 ± 3.22% ΔF/F, Test: 14.11 ± 3.25% ΔF/F, CS- Habituation: 30.96 ± 2.41% ΔF/F, Test: 18.39 ±3.21% ΔF/F). To ensure no functional group, no matter how small, was missed, Cluster 3 is also shown. For both pyramidal as well as CR-positive interneurons, this cluster contained cells whose response was increased during expression. However, in the case of VIP-positive interneurons, the third cluster contained cells whose response amplitude was similar to the habituation level (Fig. 11D, bottom panel) (CS+ Habituation: 56.95 ± 3.25% ΔF/F, Test: 18.68 ± 4.89% ΔF/F, CS Habituation: 37.33 ± 6.74% ΔF/F, Test: 21.65 ± 4.76% ΔF/F). Hence, no functional subgroup increasing their response to the CS+ could be found.

In addition, the number of responsive trials was decreased in all 3 clusters of VIP-positive interneurons (Fig. 11E). (CS+: Cluster 1: Habituation: 0.78 ± 0.08 trials, Test: 0.44 ± 0.06 trials, Wilcoxon test: $p = 0.002$. Cluster 2: Habituation: 2.71 ± 0.18 trials, Test: 1.33 ± 0.23 trials, Wilcoxon test: $p<0.0001$. Cluster 3: 1.51 ± 0.19 trials, Test: 1.21 ± 0.19 trials, Wilcoxon test: $p = 0.3$. CS-: Cluster 1: Habituation: 1.18 ± 0.10 trials, Test: 0.69 ± 0.07 trials, Wilcoxon test: $p<0.0001$. Cluster 2: Habituation: 2.00 ± 0.24 trials, Test: 1.58 ± 0.21 trials, Wilcoxon test: $p = 0.1$. Cluster 3: Habituation: 1.97 ± 0.22 trials, Test: 1.48 ± 0.16 trials, Wilcoxon test: $p = 0.012$).

These results suggest that CR interneurons increasing their response after fear conditioning are most likely VIP negative, as otherwise VIP-positive interneurons boosting their response amplitude would have been found in the VIP population. Since there are none, and the overlap with SOM is very small in our hands (see above), CR interneurons specifically increasing their response to CS+ after conditioning found in this study are most likely SOM and VIP negative.

CR-positive interneurons and pyramidal cells discriminate between CS+ and CS- during fear conditioning

The diverse effects learning can have on a neuronal population make it difficult to guess which change is important to a downstream circuit encoding behavioural reactions, especially since we found cells decreasing their response to the CS+ in both the paired and unpaired condition.

Assuming that it is important for a behavioural effector to distinguish between CS- and CS+, especially after fear conditioning, auditory system output would be expected to be different for CS- and CS+. Hence, ROC analysis of neuronal activity for different clusters and conditions was performed (see Methods).

Comparing the first trial of each tone response, the ROC curve for pyramidal cells sorted into cluster 1 fell on the 45 degree line, indicating that neuronal responses to the CS- and the CS+ are very similar and not distinguishable by a classifier (Fig. 12Ai, Aii, blue lines). Interestingly, while Cluster 2 exhibits high trial-to trial variability in separability before learning (Fig. 12Ci, Di) with no separability for the first trial, but high separability for the fourth trial, after learning it seems decreased. This higher degree of separability is due to the fact that these cells exhibit a wide range of responses to the CS-, but most of them have very small responses to the CS+ (Fig. 12Dii). The only cluster exhibiting high ROC AUC values after learning is Cluster 3, that is, cells increasing their response amplitude and decreasing their trial-to-trial variability (Fig. 12Ei, Fi).

Interestingly, by the fourth presentation of the sounds after learning, any separability that was there during the first trial, is gone (Fig. 12 Di, Fi, compare grey lines).

Figure 12: Discriminability between CS+ and CS- based on single-trial population responses of pyramidal cells. Ai: ROC curve and **Aii:** Response distributions of pyramidal cells in cluster 1 in naïve animals. Blue curve: first trial. Grey curve: fourth trial. **Bi:** ROC curve and **Bii:** Response distributions of neurons in cluster 1 after fear conditioning. **Ci:** ROC curve and **Cii:** Response distributions of neurons in cluster 2 before conditioning. **Di:** ROC curve and **Dii:** Response distributions of neurons cluster 2 after conditioning. **Ei:** ROC curve and **Eii:** Response distributions of pyramidal cells in cluster 3 in naïve animals. **Fi:** ROC curve and **Fii:** Response distribution of pyramidal cells in cluster 3 after fear conditioning. R(au): response bin size. p(R): incident count per bin (see Methods).

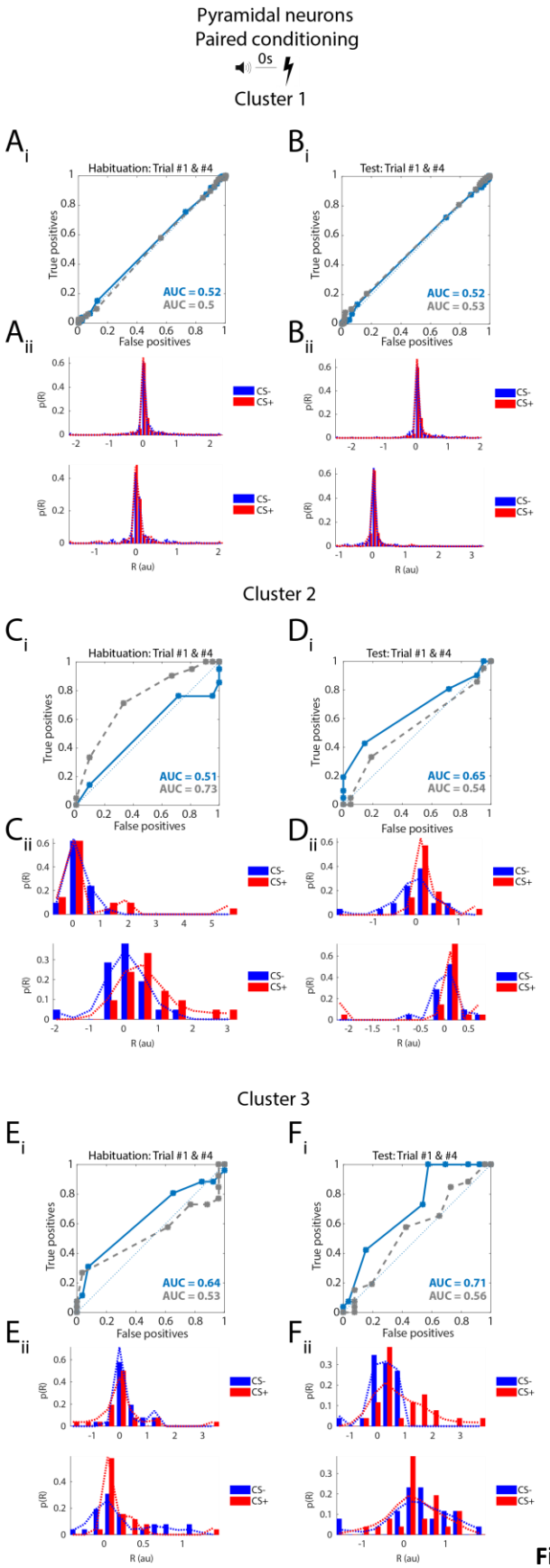
Pyramidal neurons
Paired conditioning
0s
Cluster 1
A i
Habituation: Trial #1 & #4
True positives
False positives
AUC = 0.52
AUC = 0.5
B i
Test: Trial #1 & #4
AUC = 0.52
AUC = 0.53
A ii
B ii
p(R)
CS-
CS+
R (au)
Cluster 2
C i
AUC = 0.51
AUC = 0.73
D i
AUC = 0.65
AUC = 0.54
C ii
D ii
Cluster 3
E i
AUC = 0.64
AUC = 0.53
F i
AUC = 0.71
AUC = 0.56
E ii
F ii

Figure 12

In the unpaired condition, pyramidal cells in Cluster 1 do not exhibit differential activity in response to CS- or CS+, before and after learning (Fig. 13Ai, Bi). In addition, cluster 2 cells increase their separability after learning, but to a very minor degree (Fig. 13Ci, Di). In the unpaired condition, this is true for both the first as well as the fourth trial (Fig. 13 Ai, Bi, Ci, Di, compare blue and grey lines).

Taken together, these results suggest that association of a sound with a salient outcome increases discriminability between this sound and a control sound in the auditory cortex pyramidal cells.

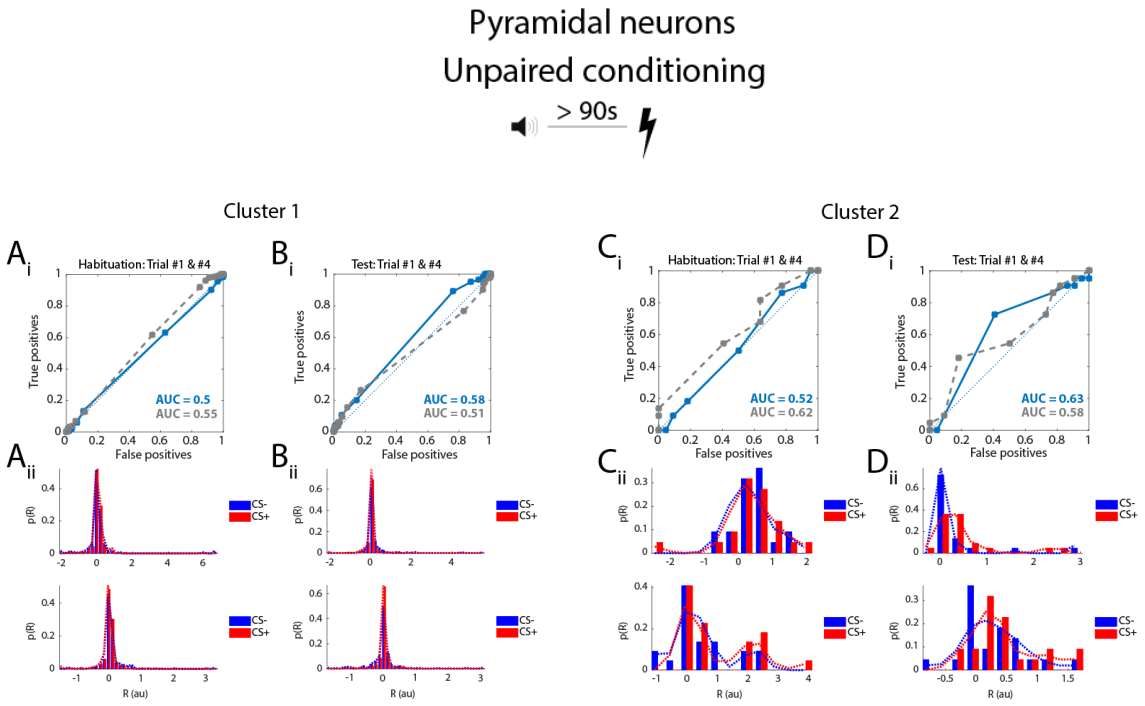

Figure 13: Discriminability between CS+ and CS- is reduced in ACX after unpaired conditioning. Ai: ROC curve and **Aii:** Response distributions of pyramidal cells in cluster 1 in naïve animals. Blue curve: first trial. Grey curve: fourth trial. **Bi:** ROC curve and **Bii:** Response distributions of neurons in cluster 1 after fear conditioning. **Ci:** ROC curve and **Cii:** Response distributions of neurons in cluster 2 before conditioning. **Di:** ROC curve and **Dii:** Response distributions of neurons cluster 2 after unpaired conditioning. R(au): response bin size. p(R): incident count per bin (see Methods).

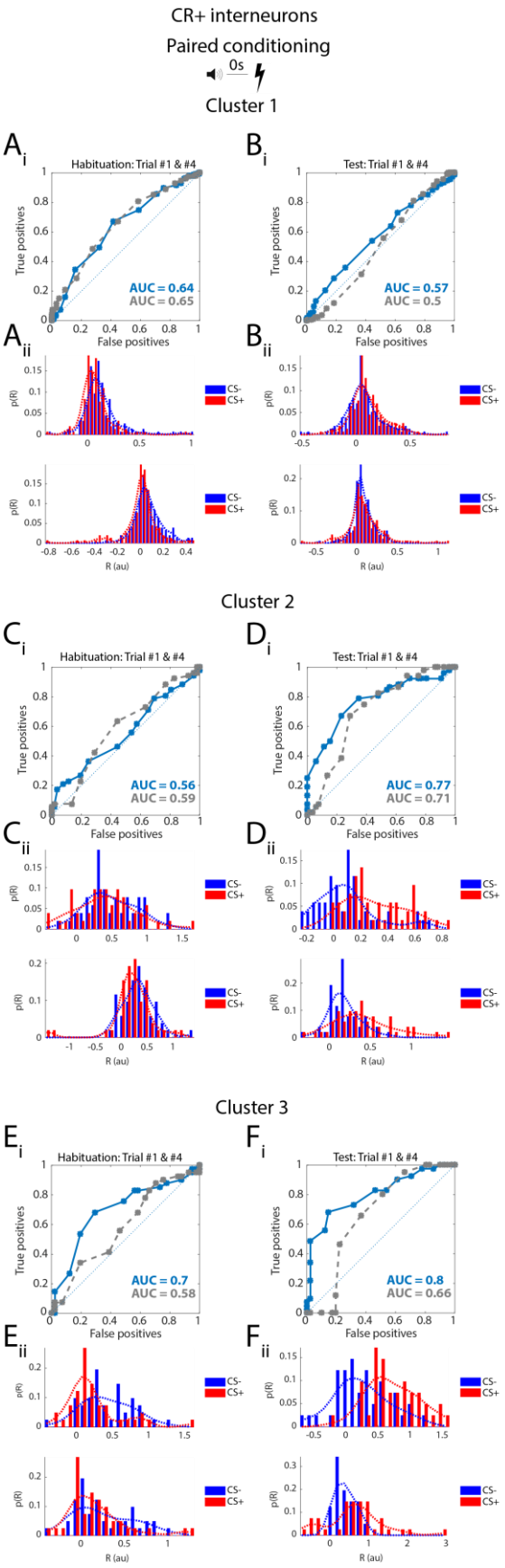
CR+ interneurons
Paired conditioning
0s
Cluster 1
A i
Habituation: Trial #1 & #4
True positives
False positives
AUC = 0.64
AUC = 0.65
B i
Test: Trial #1 & #4
AUC = 0.57
AUC = 0.5
A ii
B ii
p(R)
CS-
CS+
R (au)
Cluster 2
C i
AUC = 0.56
AUC = 0.59
D i
AUC = 0.77
AUC = 0.71
C ii
D ii
Cluster 3
E i
AUC = 0.7
AUC = 0.58
F i
AUC = 0.8
AUC = 0.66
E ii
F ii

Figure 14

Figure 14: Discriminability between CS+ and CS- is increased in 2 cluster of CR-positive interneurons during fear expression. Ai: ROC curve and **Aii:** Response distributions of CR-positive interneurons in cluster 1 in naïve animals. Blue curve: first trial. Grey curve: fourth trial. **Bi:** ROC curve and **Bii:** Response distributions of neurons in cluster 1 after fear conditioning. **Ci:** ROC curve and **Cii:** Response distributions of neurons in cluster 2 before conditioning. **Di:** ROC curve and **Dii:** Response distributions of neurons in cluster 2 after conditioning. **Ei:** ROC curve and **Eii:** Response distributions of neurons in cluster 3 in naïve animals. **Fi:** ROC curve and **Fii:** Response distribution of neurons in cluster 3 after fear conditioning. R(au): response bin size. p(R): incident count per bin (see Methods).

CR-positive interneurons in Cluster 1 exhibit some discrimination before learning, which is stable across trials (Fig. 14Ai, Aii). However, after learning, there is no separability between CS- and CS+ anymore (Fig. 14Bi, Bii). Surprisingly, cells in Cluster 2 exhibit poor discrimination before learning (Fig. 14Ci, Cii), but separability is increased after learning (Fig. 14Di, Dii). Even though this cluster contains cells that decrease their response to CS+ after learning, evoked amplitudes are still slightly larger than the ones to the CS-, making it possible for the classifier to distinguish between CS- and CS+-elicited activity (Fig. 14Dii). The highest discrimination, reflected in the size of the AUC, is exhibited by CR-positive interneurons in Cluster 3 after learning (Fig. 14Fi, Fii). Interestingly, these cells display the highest separability even before learning, showing a wide range of responses to the CS+ in naïve animals (Fig. 14Eii, red bars).

For CR-positive interneurons, as for pyramidal cells, the highest discrimination between CS- and CS+ is obtained for the first trial, and decreases with repeated exposure to the sounds, as shown by smaller AUC values for the fourth trial (Fig. 14).

In the unpaired condition, CR-positive interneurons in cluster 1 show no separability between CS- and CS+, both before and after conditioning (Fig. 15Ai, Aii, Bi, Bii). This indicates evoked activity is very similar for both sounds. Cells in cluster 2 show high discrimination between sounds before foot shock application (Fig. 15Ci, Cii), which is gone completely afterwards (Fig. 15Di, Dii). As can be seen by the binned response counts, most cells have strongly decreased their responses over the course of the experiment (Fig. 15Cii, Dii), hence making it impossible for the classifier to distinguish evoked activity.

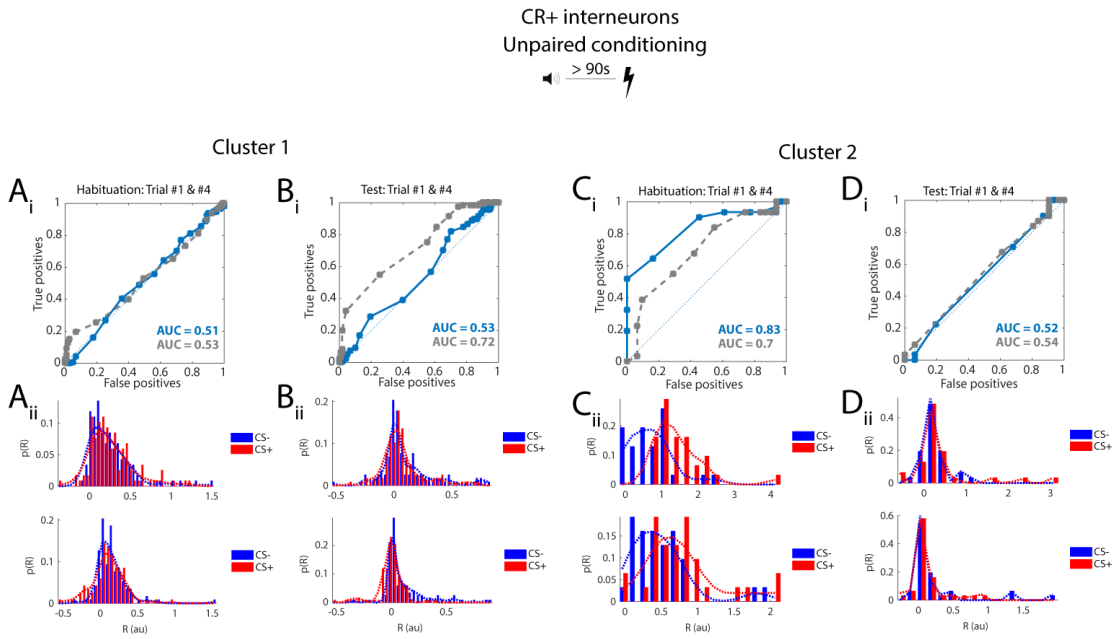

Figure 15: CR-positive interneurons do not discriminate between CS+ and CS- after unpaired conditioning. Ai: ROC curve and **Aii:** Response distributions of CR-positive interneurons in cluster 1 in naïve animals. Blue curve: first trial. Grey curve: fourth trial. **Bi:** ROC curve and **Bii:** Response distributions of neurons in cluster 1 after unpaired conditioning. **Ci:** ROC curve and **Cii:** Response distributions of neurons in cluster 2 before conditioning. **Di:** ROC curve and **Dii:** Response distributions of neurons in cluster 2 after unpaired conditioning. R(au): response bin size. p(R): incident count per bin (see Methods).

In summary, it becomes clear that fear conditioning improves the separability of the CS+-elicited activity from the activity caused by a neutral control tone. In addition, even cells for which the population average looks very similar (comparing Cluster 2 of the paired and unpaired conditioning of CR-positive interneurons), the underlying population response can be very diverse.

Interestingly, cells sorted into Cluster 3 for both pyramidal neurons and CR-positive interneurons appear to be better at discriminating CS+ and CS- even before fear conditioning. This could hint at good sound discrimination potentially being a selection criteria for cells to be recruited during the learning process.

VIP-positive interneurons in Cluster 1 exhibit poor discrimination between CS- and CS+, which is slightly increased after conditioning (Fig. 16Ai, Aii, Bi, Bii). VIP-positive interneurons in cluster 2 discriminate well between CS- and CS+ before conditioning (Fig. 16Ci, Cii), however, after

learning, this discrimination is markedly reduced (Fig. 16Di, Dii). As could be observed for the other neurons, there is a decrease in separability for the fourth trial (Fig. 16). The exception is Cluster 2 before learning. The latter appears to be due to cells decreasing their responses to both stimuli overall, but maintaining relative response proportions (Fig. 16Cii).

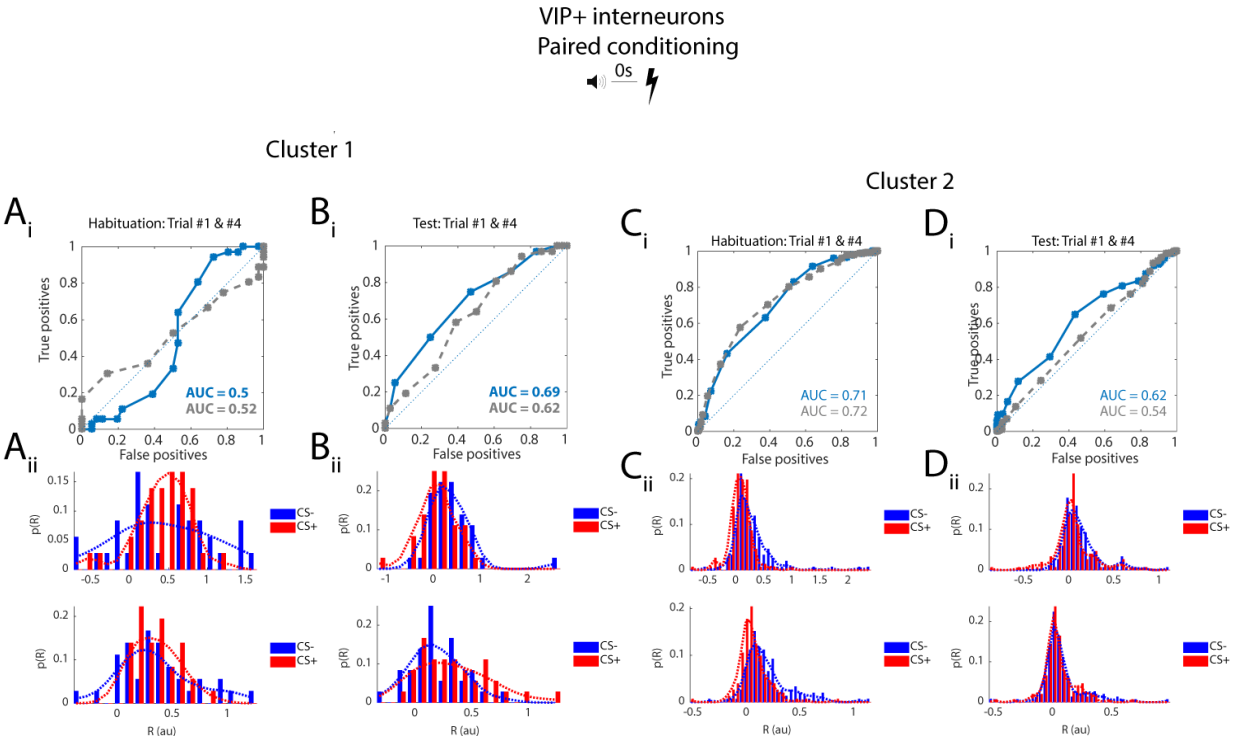

Figure 16: VIP-positive interneurons exhibit poor discrimination between both CS after fear conditioning. Ai: ROC curve and **Aii:** Response distributions of VIP-positive interneurons in cluster 1 in naïve animals. Blue curve: first trial. Grey curve: fourth trial. **Bi:** ROC curve and **Bii:** Response distributions of neurons in cluster 1 after fear conditioning. **Ci:** ROC curve and **Cii:** Response distributions of neurons in cluster 2 before conditioning. **Di:** ROC curve and **Dii:** Response distributions of neurons in cluster 2 after conditioning. R(au): response bin size. p(R): incident count per bin (see Methods).

Altered response dynamics in ACX after conditioning are not due to animal motion

During imaging of auditory cortex activity, the animals were free to run on a spherical treadmill (see Methods). Auditory cortex has been shown to receive both cholinergic input related to animal motion as well as corollary discharge from motor cortex (Schneider et al, 2014). To make sure the plasticity effects observed in paired groups are due to the conditioning protocol and not due to differences in running behaviour of the animals, the number of CS presentations spent running was evaluated for each group (Fig. 17). For all the interneuron groups, the animals spend slightly more CS+ trials running then the CS- trials after conditioning (Fig. 17B), however, the difference is not significant. Importantly, there are no differences between the CS+ presentations of paired and unpaired interneuron group. Hence, differences in CS+ evoked responses are most likely not due to differences in running activity.

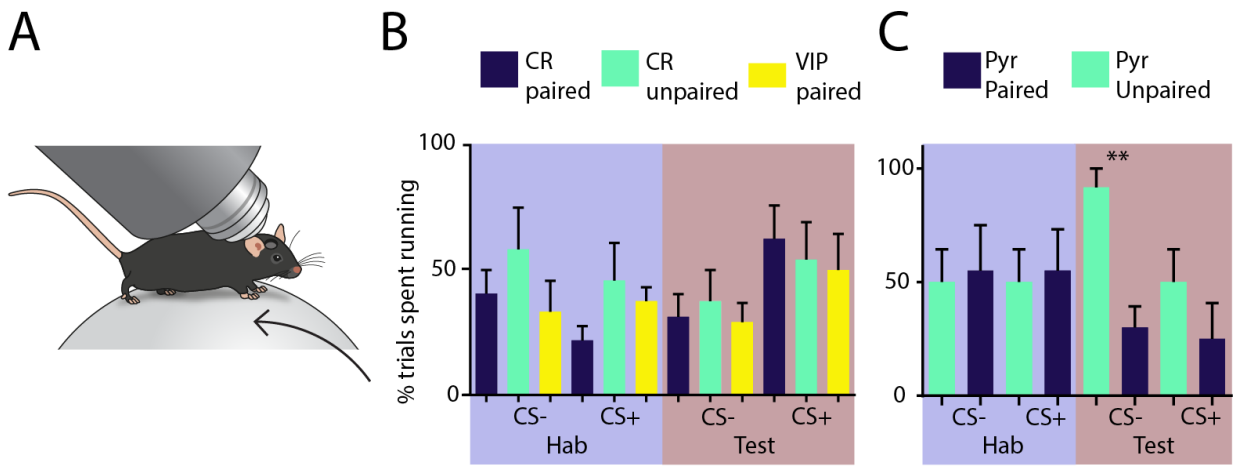

Figure 17: Altered response dynamics are not due to animal motion suppressing neuronal activity in ACX. A: Scheme of the animal running on the Styrofoam treadmill. **B:** Amount of trials during which the animal exhibited any locomotion activity for all interneuron groups. **C:** Amount of trials during which the animal exhibited any locomotion activity for pyramidal cells. Bars: Mean, Error bars: SEM. CS- pyramidals: Unpaired t-test, p = 0.004.

For pyramidal cells, no differences were found in the amount of running trials for CS+ between paired and unpaired animals (Fig. 17B). While there was a significant increase measured for CS- trials for unpaired animals, differences between evoked population responses were found only

for the CS+ trials. Therefore, these differences are most likely not due to increased or decreased animal locomotion.

Discussion

Examining pyramidal cells and CR-positive interneurons during fear expression revealed subpopulations within each cell type which specifically increased their responses to the CS+. Additionally, evoked responses of these cells become more reliable, indicating a decreased trial-to-trial variability. Both subpopulations were absent from a control group, in which animals did not form the sound-foot shock association.

Notably, for both the paired and the unpaired condition, CR-positive interneurons as well as pyramidal cells decreasing their sound-evoked response were found. These cells decreased the number of trials they responded to over the course of the experiment, effectively increasing their trial-to-trial variability. In addition, VIP-positive interneurons, which overlap significantly with the CR-positive interneuron population, did not show a CS+-specific increase in response size. Hence, CR-positive interneurons increasing their CS+-evoked response are most likely VIP negative.

ROC analysis showed that cells increasing their CS+-evoked response also increased their ability to discriminate between CS+ and CS- after conditioning. This indicates that CS- and CS+ evoke differential responses in those neuronal populations. Interestingly, even CR-positive interneurons decreasing their response to the CS+ after conditioning still exhibit good discrimination, whereas pyramidal cells of that group do not exhibit similarly strong differential activation. Additionally, poor discrimination was found for VIP-positive interneurons during fear expression.

Taken together, these results suggest the existence of a microcircuit in layer 2/3 of auditory cortex involving a subpopulation of pyramidal cells and CR-positive, VIP-negative interneurons. This microcircuit appears to be mediating strong CS+-specific activation during fear expression to downstream targets.

Pupil size as a proxy for fear

Freely-moving mice typically display explorative behaviour in a neutral context, and freeze when presented with fearful stimuli (see Introduction). Head fixation inhibits the natural explorative behaviour of mice, even when they are allowed to run freely on a treadmill. Hence, immobility occurs frequently during the experiment, making it impossible to distinguish freezing.

Measuring freezing levels and pupil dilations in the same group of fear conditioned animals showed a strong correlation between both measures, as has been observed previously (Oleson et al, 1972, Lennartz & Weinberger, 1992). Notably, pupil dilations occur specifically in response to the conditioned stimulus. In an unpaired control paradigm, mice did not form an association between the sound and the foot shock, and increased pupil dilations in response to sounds were absent.

However, pupil size is not only an indicator of fear. Cortical state changes, such as transitioning between quiet wakefulness and running, are closely tracked by pupil size (Reimer et al, 2014, Harris & Thiele, 2011), as is sympathetic network tone (Bradley et al, 2008). Additionally, cholinergic signaling preceding movement initiation was correlated with pupil size (Nelson & Mooney, 2016).

To ensure that the differences observed in pupil size between paired und unpaired groups, as well as between CS+ and CS-, were due to differences in fear level and not due to differences in locomotion, the number of trials during which the animal was running were quantified. The number of CS+ trials spent running does not differ between the interneuron groups, indicating that the differences in pupil size observed between paired and unpaired CS+ presentation are unlikely to be a result of pupil activity correlated to running onset. There is a slight increase in the number of trials spent running between CS- trials and CS+ trials, but this difference is not significant for any interneuron group. The relative increase is very similar between paired and unpaired conditioning, therefore it is unlikely that differences in pupil dilation are due to differences in locomotion.

No differences in the number of trials running was found for animals in the paired pyramidal cells group. However, animals in the unpaired pyramidal cells group spent a large number of trials running, significantly more than during the CS+ presentation. Importantly, quantification of pupil size was strictly limited to sound onset. Locomotion onset was never correlated to sound onset, hence no significant difference between pupil sizes for CS- trials was found.

In summary, pupil dilation in response to a discrete stimulus is a good proxy for measuring fear levels in a head-fixed animal.

Auditory cortex – Tuning

According to previous findings, pyramidal cells in auditory cortex are narrowly tuned, and interneurons tend to be widely tuned (Wu et al, 2008, Li et al, 2014). Measuring tuning at the imaging sites used in this study found very similar tuning distributions. Pyramidal cells are narrowly tuned to a specific frequency area, while both interneuron populations investigated here respond to more frequencies. All cell groups covered the whole frequency spectrum tested, with roughly equal numbers of cells responding to different frequency areas.

The age of the animals used in this study has to be taken into account when interpreting the tuning results. C57/Bl6 animals lose high frequency sensitivity during their lifetime (Willott et al, 1993, Brewton et al, 2016). At 3 months of age, higher frequency sensitivity begins to disappear in favour of frequencies in the range of 10-12 kHz (Willott et al, 1993). Mice used in this study are on average 3 months old, which might be why higher frequencies are not overrepresented in this dataset.

On a large scale across primary auditory cortex and secondary auditory fields, frequencies are tonotopically organized, whereas local circuits do not show tonotopic organization (Stiebler et al, 1997, Rothschild et al, 2010, Bandyopadhyay et al, 2010). Therefore, observing cells tuned to different frequencies in the same field of view was expected.

Auditory fear conditioning induces long-lasting plasticity in ACX

Previous studies have shown plasticity in ACX upon auditory fear conditioning (Dimyan & Weinberger, 1999, Quirk et al, 1997, Kuchibhotla, 2016). These studies generally focused on pyramidal cells. A subpopulation of pyramidal cells imaged in this study increased their response specifically to the CS+, both in amplitude as well as in the number of trials they respond to. A binary classifier was able to distinguish between CS+ and CS- based on the neuronal responses of this subpopulation. Furthermore, the ROC analysis indicated that these cells already discriminated well between both sounds before conditioning. This subpopulation follows the classical view of expansion of responses to the CS+ in ACX (Weinberger, 2004). Increasing response strengths leads to an increased number of spikes fired in response to the CS+, which is believed to increase the signal-to-noise ratio for salient stimuli. Notably, similar cells could not be found in the unpaired group, hence it appears that this form of plasticity is specific for the CS+, and is only present during fear expression in animals actually conditioned to that specific sound.

Interestingly, CR-positive interneurons modulating their response in a similar way were found in animals of the paired conditioned group. About 20% of CR interneurons increased their response to the CS+, a larger percentage than in the pyramidal neuron group (8%). Similarly, these cells also increased their number of responsive trials. ROC analysis showed that these cells discriminate very well between both CS before conditioning, and even increase discriminability during fear expression.

Taken together, these results suggest the existence of a disinhibitory circuit formed by these two subpopulations. Caputi et al (2009) have shown that CR-positive interneurons form functional synaptic connections onto PV-positive interneurons. Therefore, an increase in activity of CR-positive interneurons might lead to increased inhibition of PV-positive interneurons. This in turn would release pyramidal cells from inhibition, allowing them to respond strongly to sounds. Preliminary optogenetic experiments suggest that this might indeed be the case, as light activation of CR-positive interneurons lead to an average increase in the calcium signal of pyramidal cells (preliminary experiments). Further experiments will have to confirm whether

functional connections between CR- and PV-positive interneurons do exist in ACX and are involved in mediating these plasticity effects.

Plasticity – adaptation to non-salient stimuli

In both the paired and the unpaired group, pyramidal cells decreasing their response to the CS+ during fear expression could be found. These cells exhibited a very strong sound response to both the CS+ and the CS- before conditioning in both groups. Over the course of the experiment, the trial-to-trial variability increased in these neurons. Additionally, discriminability between CS+ and CS- was overall low for those cells.

The decay of evoked amplitude is similar to what Kato et al. observed during their habituation paradigm (Kato et al, 2015). At least in the unpaired group, these data suggest that the auditory system adapts to behaviourally irrelevant sounds and eventually ignores them. However, this conclusion cannot easily be extended to the cells decreasing their amplitude in the paired group. Neurons decreasing their amplitude to conditioned sounds have been described before, (Dimyan & Weinberger, 1999, Kato et al, 2015, Kuchibhotla et al, 2016), the meaning of it remains elusive. One might speculate to the existence of a pyramidal subnetwork encoding novel auditory stimuli, which would decrease its responses after several exposures, whether the stimulus gains saliency or not. Finding pyramidal cells which decrease their response amplitude in the paired and unpaired condition might hint at this possibility. However, another hypothesis might be the existence of a pyramidal subnetwork targeting output structures not needed in the fear conditioning paradigm. Currently, tagging or identifying potential pyramidal subnetworks is very difficult, hence little is known about the diversity of the largest cell group in cortical layer 2/3. Further advances in identifying functionally connected pyramidal subnetworks will be crucial to fully understand cortical function and integration.

In addition, within-session habituation was observed in pyramidal cells as well. While CS+ and CS- were well discriminated by pyramidal cells in cluster 3 during the first CS+ trial, by trial 4, this discrimination has disappeared. Evoked responses within the same session after trial 4 become

smaller and smaller (unpublished observation), even though fear memory is typically not extinguished by 4 presentations of the CS+ (Herry et al, 2008, Whittle et al, 2013). The meaning of this within-session habituation remains to be understood.

Similarly, a subpopulation of CR interneurons decreases their response to the CS+ in both the paired and the unpaired condition. However, CR-positive interneurons decreasing their responses are still able to discriminate well between CS+ and CS-, as the absolute response amplitudes evoked by both sounds remains different. In the unpaired condition, these cells are not able to differentiate between sounds after conditioning. This raises the possibility that CR-positive interneurons decreasing their amplitude after paired conditioning do so in a graded manner, and still might contribute to differential encoding. Indeed, the degree of amplitude reduction might be crucial to downstream encoding. Paired recordings in the neocortex showed that CR-positive interneurons are heavily interconnected (Caputi et al, 2009), suggesting that a stimulus-specific decrease in inhibition might disinhibit another part of the CR-positive population. Further experiments exploring the functional connectivity of these interneurons will have to confirm this notion.

Plasticity – Reduction of evoked responses due to animal motion

As detailed in the introduction, different behavioural states influence sensory encoding. During running, ACX responses are typically reduced (Zhou et al, 2014). To ensure changes of evoked responses were actually due to learning-induced plasticity and not due increased animal motion, the number of trials the animal spent running were analyzed. In the interneuron groups, there was a slight increase in the number of trials spent running during CS+ presentation compared to CS- presentations, but this difference was not significant. Interestingly, an increase in evoked responses was only found for the CS+, indicating that this change in amplitude cannot be related to the increase in animal motion, as that would suppress this activity. For pyramidal cells, the paired group had no differences in running episodes between CS- and CS+. The unpaired group however had a significant decrease in time spent running during the CS+. According to previous findings, evoked responses should therefore on average be increased for the CS+ during those

trials. However, the exact opposite was found. Therefore, changes in sound-evoked responses between habituation and test are most likely no due to changes in locomotion.

Discriminability between CS+ and CS- is increased during fear expression

For a mouse to adjust its behaviour according to different stimuli in its environment, it has to successfully identify behaviourally salient stimuli and discriminate them from meaningless ones. One expectation of a system successfully representing those stimuli would be that their evoked responses are different enough for an unbiased observer to distinguish between them. This is exactly what a ROC analysis reports. While only pyramidal cells selectively increasing their response to the CS+ exhibit good discrimination between CS+ and CS- after learning, CR- interneurons both increasing and decreasing their responses show good discrimination. Taken together, these results would indicate that indeed, discriminability is enhanced after fear learning. In addition, it appears as if only cells that already discriminate between both sounds before fear conditioning would selected for response enhancement. This may be seen as further evidence that cells increasing their evoked responses might form a cortical microcircuit, potentially targeting downstream structures requiring salient stimulus information, such as the amygdala. Previously, ACX has been shown to form discrete perceptual categories for salient and non-salient sounds (Bathellier et al, 2012), with local neuronal populations being able to discriminate sound based on behavioural relevancy. Whether the responses observed here fit into one of these discrete categories remains an open question, but the ROC analysis indicates that in principle, response amplitudes of the neuronal populations are different enough for an unbiased observer to discriminate between CS+ and CS-.

Combining insights into CR-positive interneurons with insights into layer 1 interneurons

As mentioned in the introduction, the molecular identity of layer 1 interneurons mediating foot shock-evoked disinhibition is undefined (Letzkus et al, 2011). Previous studies have identified CR, VIP, NPY and, to a small degree, SOM as molecular markers being expressed in cortical layer 1 (Xu et al, 2010).

Functionally, VIP-positive interneurons have been found to be responsive to both rewards and punishments (Pi et al, 2013), which are presumably mediated by cholinergic signaling from the basal forebrain (Hasselmo, 2006, Weinberger, 2007). Furthermore, VIP-positive interneurons are modulated by cholinergic signaling preceding locomotion onset (Fu et al, 2014). Interestingly, CR-positive interneurons also express nicotinic receptors, and can therefore be activated by cholinergic signaling (Porter et al, 1999). Taken together, layer 1 interneurons mediating foot shock responses might be VIP-positive (Poorthuis et al, 2014). Considering the fact that CR-positive interneurons have been shown to target PV-positive interneurons (Caputi et al, 2009), foot-shock excited layer 1 interneurons might also be CR-positive.

Why do VIP-interneurons not increase their response to the CS+ during fear memory expression? In this dataset, the CS+- evoked response of VIP-interneurons is markedly reduced compared to the CR-positive interneurons. Looking at the time course of the evoked response of VIP-positive interneurons, it becomes obvious that some of these cells display a delayed, albeit reduced in amplitude, response to the CS+. Since the foot shock is applied at the end of the CS+, VIP-positive interneurons might shift their response to the time point of the expected pain. On the other hand, in visual cortex, increased decorrelation of interneuron responses has been found after a learning task (Poort et al, 2016). Another possible hypothesis is that while VIP-positive interneurons signal the actual arrival of the foot shock, during fear expression, no actual foot shock is applied. Another interneuron population, potentially CR-positive interneurons, might take over, and disinhibit pyramidal cells. If that was the case, VIP-positive interneurons would function as gate keepers, but the memory would be kept in CR-positive interneurons. However, CR-positive interneuron activity during fear acquisition is unknown. Further experiments will

have to be conducted to fully elucidate the interplay between both those interneuron subtypes and their respective contributions to fear acquisition and fear expression.

Disinhibition of pyramidal cells during fear acquisition was shown to be crucial for the formation of fear memories, when using complex sounds as CS+ (Letzkus et al, 2011). Further studies have corroborated that ACX is critically involved in fear acquisition and expression (Wigestrand et al, 2016), and additionally even for consolidation of recent fear memories (Cambiaghi, 2016b).

Summary

Layer 1 interneurons in ACX mediate crucial foot-shock information during fear acquisition, leading to disinhibition of selected pyramidal cells via PV-positive interneurons. During fear expression, previously conditioned sounds evoked strong responses in a subset of pyramidal neurons and CR-positive interneurons, implying the existence of a dinshibitory microcircuit mediating salient sound responses after conditoning. Auditory cortex has been shown to be necessary for auditory fear conditioning, implying that the observed plastic changes in the cortical circuit are driving fear behaviour during CS+ exposure. Auditory cortex might therefore play a vital role in instructing downstream brain areas about saliency of sound stimuli.

Outlook

Further experiments will be needed to determine the exact functional connectivity of CR-interneurons and other interneurons in ACX. Preliminary data suggests that optogenetically activating CR-positive interneurons leads to excitation in pyramidal cells. Combining optogenetic activation of CR-positive interneurons with sound stimulation strongly increases the sound response in pyramidal cells compared to control conditions. This finding has to be confirmed, and substantiated by obtaining the connectivity of CR interneurons. Furthermore, even though CR-

positive interneurons have been shown to express nicotinic receptors (Porter et al, 1999), their in vivo response to cholinergic stimulation remains elusive.

Cholinergic signaling has been shown to mediate foot shock information during fear conditioning, however, it should be investigated whether it also drives interneurons during fear expression. In addition, acetylcholine is unlikely to be the only neuromodulator driving plastic changes during fear conditioning and fear expression. Cortical interneurons have also been shown to respond to other neuromodulators, such as serotonin (Lee et al, 2010), and even to endocannabinoids (Bacci et al, 2004), whose roles in ACX plasticity during fear conditioning is not defined.

While calcium indicators still lack temporal precision, they nevertheless allow for the recording of the activity of large populations of neurons in behaving animals. The challenge ahead lies in understanding the complex response patterns and interactions found in these datasets. Applying principles gained from research into machine learning and 'big data' to neuronal population data will bring neuroscientists closer to understanding how information is encoded in the brain.

References

Antunes, R., and M. A. Moita

2010 Discriminative Auditory Fear Learning Requires Both Tuned and Nontuned Auditory Pathways to the Amygdala. Journal of Neuroscience 30(29):9782-9787.

Atiani, Serin, et al.

2009 Task Difficulty and Performance Induce Diverse Adaptive Patterns in Gain and Shape of Primary Auditory Cortical Receptive Fields. Neuron 61(3):467-480.

Bacci, Alberto, John R. Huguenard, and David A. Prince

2004 Long-lasting self-inhibition of neocortical interneurons mediated by endocannabinoids. Nature 431(September):1-5.

Bakin, Jonathan S., and Norman M. Weinberger

1990 Classical conditioning induces CS-specific receptive field plasticity in the auditory cortex of the guinea pig. Pp. 271-286, Vol. 536.

Bandyopadhyay, Sharba, Shihab A. Shamma, and Patrick O. Kanold

2010 Dichotomy of functional organization in the mouse auditory cortex. Nat Neurosci 13(3):361-368.

Bao, Shaowen, et al.

2004 Temporal plasticity in the primary auditory cortex induced by operant perceptual learning. Nature neuroscience 7(9):974-81.

Bathellier, Brice, Lyubov Ushakova, and Simon Rumpel

2012 Discrete Neocortical Dynamics Predict Behavioral Categorization of Sounds. Neuron 76(2):435-449.

Bradley, M. B., et al.

2008 The pupil as a measure of emotional arousal and automatic activation. Psychophysiology 45(4):602-602.

Brewton, Dustin H., et al.

2016 Age-Related Deterioration of Perineuronal Nets in the Primary Auditory Cortex of Mice. Frontiers in Aging Neuroscience 8(November):270-270.

Cambiaghi, Marco, et al.

2016 Differential Recruitment of Auditory Cortices in the Consolidation of Recent Auditory Fearful Memories. The Journal of Neuroscience 36(33):8586-8597.

Caputi, Antonio, et al.

2009 Two calretinin-positive gabaergic cell types in layer 2/3 of the mouse neocortex provide different forms of inhibition. Cerebral Cortex 19(6):1345-1359.

Chen, I. Wen, Fritjof Helmchen, and Henry Lütcke

2015 Specific Early and Late Oddball-Evoked Responses in Excitatory and Inhibitory Neurons of Mouse Auditory Cortex. The Journal of neuroscience : the official journal of the Society for Neuroscience 35(36):12560-73.

Christianson, G. Björn, Maneesh Sahani, and Jennifer F. Linden

2011 Depth-Dependent Temporal Response Properties in Core Auditory Cortex. Journal of Neuroscience 31(36):12837-12848.

Christophe, E., et al.

2002 Two types of nicotinic receptors mediate an excitation of neocortical layer I interneurons. Journal of Neurophysiology 88(3):1318-1327.

Chu, Zhiguo, Mario Galarreta, and Shaul Hestrin

2003 Synaptic Interactions of Late-Spiking Neocortical Neurons in Layer 1. 23(1):96-102.

Dekker A.J., Langdon D.J., Gage F.H., Thal L.J.

1991 NGF increases cortical acetylcholine release in rats with lesions of the nucleus basalis. Neuroreport. 1991 Oct;2(10):577-80.

Deneve, S., P. E. Latham, and A. Pouget

1999 Reading population codes: a neural implementation of ideal observers. Nature neuroscience 2(8):740-5.

DiCara LV, Braun JJ, Pappas BA.

Classical conditioning and instrumental learning of cardiac and gastrointestinal responses following removal of neocortex in the rat. J Comp Physiol Psychol. 1970 Nov;73(2):208-16.

Dimyan, Michael A., and Norman M. Weinberger

1999 Basal forebrain stimulation induces discriminative receptive field plasticity in the auditory cortex. Behav Neurosci 113(4):691-702.

Dombeck, Daniel a, et al.

2007 Imaging Large-Scale Neural Activity with Cellular Resolution in Awake, Mobile Mice. Neuron 56(1):43-57.

Fanselow, Michael S., and Andrew M. Poulos

2005 T HE N EUROSCIENCE OF M AMMALIAN A SSOCIATIVE L EARNING.

Fu, Yu, et al.

2015 A cortical disinhibitory circuit for enhancing adult plasticity. eLife 2015(4):1-12.

Galambos, R., G. Sheatz, and V. G. Vernier

1956 Electrophysiological Correlates of a Conditioned Response in Cats. Science 123(3192):376-7.

Gonchar, Y., and A. Burkhalter

1999 Connectivity of GABAergic Calretinin-immunoreactive Neurons in Rat Primary Visual Cortex. Cerebral Cortex 9(7):683-696.

Grosso, A., et al.

2015 Auditory cortex involvement in emotional learning and memory. Neuroscience 299:45-55.

Group, The Petilla Interneuron Nomenclature

2008 Petilla terminology: nomenclatures of features of GABAergic interneurons of the cerebral cortex. Nature Reviews Neuroscience 9(7):557-568.

Gulledge, Allan T., et al.

2007 Heterogeneity of phasic cholinergic signaling in neocortical neurons. Journal of neurophysiology 97(3):2215-29.

Harris, Kenneth D.

2012 Cell Assemblies of the Superficial Cortex. Neuron 76(2):263-265.

Harris, Kenneth D., et al.

2011 How do neurons work together? Lessons from auditory cortex. Hearing Research 271(1-2):37-53.

Harris, Kenneth D., and Thomas D. Mrsic-flogel

2013 Cortical connectivity and sensory coding. Nature 503(7474):51-58.

Harris, Kenneth D., and Gordon M. G. Shepherd

2015 The neocortical circuit: themes and variations. Nature Neuroscience 18(2):170-181.

Harris, K. D., and A. Thiele

2011 Cortical state and attention. Nat Rev Neurosci 12(9):509-523.

Hars B., Maho C., Edeline, J.-M., Hennevin E.

Basal forebrain stimulation facilitates tone-evoked responses in the auditory cortex of awake rat. Neuroscience, Volume 56, Issue 1, September 1993, Pages 61–74

Hasselmo, Michael E.

2006 The role of acetylcholine in learning and memory. Current Opinion in Neurobiology 16(6):710-715.

Herry, Cyril, et al.

2008 Switching on and off fear by distinct neuronal circuits. Nature 454(7204):600-606.

Hudspeth, A. J.

1989 How the ear's works work. Nature 341(6241):397-404.

Jiang, Xiaolong, et al.

2013 The organization of two new cortical interneuronal circuits. Nature neuroscience 16(2):210-8.

Kato, Hiroyuki K., Shea N. Gillet, and Jeffry S. Isaacson

2015 Flexible Sensory Representations in Auditory Cortex Driven by Behavioral Relevance. Neuron 88(5):1027-1039.

Kawaguchi, Yasuo, et al.

2010 Selective Cholinergic Modulation of Cortical GABAergic Cell Subtypes Selective Cholinergic Modulation of Cortical GABAergic Cell Subtypes.1743-1747.

Kawaguchi, Y., and Y. Kubota

1996 Physiological and morphological identification of somatostatin- or vasoactive intestinal polypeptide-containing cells among GABAergic cell subtypes in rat frontal cortex. The Journal of neuroscience: the official journal of the Society for Neuroscience 16(8):2701-2715.

Kuchibhotla, Kishore V., et al.

2016 Parallel processing by cortical inhibition enables context-dependent behavior. Nature Neuroscience (October):1-14.

Latham, Peter E., and Yasser Roudi

2010 Population Coding. (C):6-7.

LeDoux, Joseph E.

2000 Emotion circuits in the Brain. Annual Review of Neuroscience 23:155-184.

Lee, Soohyun, et al.

2010 The Largest Group of Superficial Neocortical GABAergic Interneurons Expresses Ionotropic Serotonin Receptors. 30(50):16796-16808.

Lennartz, Robert C., and Norman M. Weinberger

1992 Analysis of response systems in Pavlovian conditioning reveals rapidly versus slowly acquired conditioned responses: Support for two factors , implications for behavior and neurobiology. 20(2):93-119.

Li, Ling-Yun, et al.

2014 Differential Receptive Field Properties of Parvalbumin and Somatostatin Inhibitory Neurons in Mouse Auditory Cortex. Cerebral cortex (New York, N.Y. : 1991) 14(July):bht417--bht417-.

Letzkus J.J., Wolff S.B.E., Meyer E.M.M., Tovote P., Courtin J., Herry C., Luthi A.

2011 A disinhibitory microcircuit for associative fear learning in the auditory cortex. Nature 480(7377): 331:335

Maren, Stephen

2001 Neurobiology of Pavlovian Fear Conditioning. Annual Review of Neuroscience 24:897-931.

Mayford, Mark, Steven A. Siegelbaum, and Eric R. Kandel

2012 Synapses and Memory Storage. Cold Spring Harb Perspect Biol 4(6):1-18.

McDonald, Robert J., Bryan D. Devan, and Nancy S. Hong

2004 Multiple memory systems: The power of interactions. Neurobiology of Learning and Memory 82(3):333-346.

McKenna T.M., Ashe J.H., Hui G.K., Weinberger N.M.

Muscarinic agonists modulate spontaneous and evoked unit discharge in auditory cortex of cat. Synapse. 1988;2(1):54-68.

Milner, Brenda, Larry R. Squire, and Eric R. Kandel

1998 Cognitive Neuroscience Review and the Study of Memory. Neuron 20:445-468.

Moore, A. K., and M. Wehr

2013 Parvalbumin-Expressing Inhibitory Interneurons in Auditory Cortex Are Well-Tuned for Frequency. Journal of Neuroscience 33(34):13713-13723.

Nabavi, Sadegh, et al.

2014 Engineering a memory with LTD and LTP. Nature 511(7509):348-352.

Nelson, Anders, et al.

2016 The Basal Forebrain and Motor Cortex Provide Convergent yet Distinct Movement-Related Inputs to the Auditory Cortex Article The Basal Forebrain and Motor Cortex Provide Convergent yet Distinct Movement-Related Inputs to the Auditory Cortex. Neuron 90(3):1-14.

Oleson, T., Westenberg, I., Weinberger N.M.

1972 Characteristics of the pupillary dilation response during pavlovian conditioning in paralyzed cats. Behavioral Biology 7(6): 829-840

Otazu, Gonzalo H., et al.

2009 Engaging in an auditory task suppresses responses in auditory cortex. Nature neuroscience 12(5):646-654.

Pi, Hyun-Jae, et al.

2013 Cortical interneurons that specialize in disinhibitory control. Nature 503(7477):521-4.

Polley, Daniel B., et al.

2004 Associative learning shapes the neural code for stimulus magnitude in primary auditory cortex. Proceedings of the National Academy of Sciences of the United States of America 101(46):16351-6.

Poort,J., Khan A.G., Blot A., Hofer S.B., Mrsic-Flogel, T.D.

2016 Learning changes the selectivity and interactions of GABAergic interneuron classes in visual cortex

Abstract at SFN Meeting 2016, 433.19 / SS3

Poorthuis, Rogier B., Leona Enke, and Johannes J. Letzkus

2014 Cholinergic circuit modulation through differential recruitment of neocortical interneuron types during behaviour. The Journal of physiology 592(Pt 19):4155-64.

Porter, J. T., et al.

1999 Selective excitation of subtypes of neocortical interneurons by nicotinic receptors. The Journal of neuroscience: the official journal of the Society for Neuroscience 19(13):5228-5235.

Pouget, Alexandre, Peter Dayan, and Richard S. Zemel

2003 Inference and computation with population codes. Annual Review of Neuroscience 26(1):381-410.

Quian Quiroga, Rodrigo, and Stefano Panzeri

2009 Extracting information from neuronal populations: information theory and decoding approaches. Nature reviews. Neuroscience 10(MArCH):173-185.

Quirk, Gregory J., Jorge L. Armony, and Joseph E. LeDoux

1997 Fear conditioning enhances different temporal components of tone-evoked spike trains in auditory cortex and lateral amygdala. Neuron 19(3):613-624.

Quiroga, Rodrigo Quian, and Stefano Panzeri

2013 Decoding and Information Theory in Neuroscience. Principles of Neural Coding.

Reimer, Jacob, et al.

2014 Pupil Fluctuations Track Fast Switching of Cortical States during Quiet Wakefulness. Neuron 84(2):355-362.

Richardson, R. T., and M. R. DeLong

1990 Context-dependent responses of primate nucleus basalis neurons in a go/no-go task. The Journal of neuroscience: the official journal of the Society for Neuroscience 10(8):2528-2540.

Romanski L.M., LeDoux J.E

1992 Bilateral destruction of neocortical and perirhinal projection targets of the acoustic thalamus does not disrupt auditory fear conditioning. Neuroscience Letters, Volume 142, Issue 2, Pages 228–232

Romanski L.M., LeDoux J.E.

1993 Information cascade from primary auditory cortex to the amygdala: corticocortical and corticoamygdaloid projections of temporal cortex in the rat. Cereb Cortex 3(6):515-32.

Romanski, L. M., Clugnet, M.,; Bordi, F.,; LeDoux, J. E.

1993 Somatosensory and auditory convergence in the lateral nucleus of the amygdala.

Behavioral Neuroscience, Vol 107(3): 444-450.

Rothschild, Gideon, Israel Nelken, and Adi Mizrahi

2010 Functional organization and population dynamics in the mouse primary auditory cortex. Nature neuroscience 13(3):353-360.

Rudy, Bernardo, et al.

2010 Three groups of interneurons account for nearly 100% of neocortical GABAergic neurons. Developmental Neurobiology 71(1):45-61.

Sanger, T. D.

1996 Probability density estimation for the interpretation of neural population codes. Journal of neurophysiology 76(4):2790-2793.

Sanger, Terence D.

2003 Neural population codes. Current Opinion in Neurobiology 13:238-249.

Schindelin, Johannes, et al.

2012 Fiji: an open-source platform for biological-image analysis. Nature Methods 9(7):676-682.

Schreiner, Christoph E., and Jeffery A. Winer

2007 Auditory cortex mapmaking: principles, projections, and plasticity. Neuron 56(2):356-65.

Smith, P.H.,Spirou G.A.

2002 From the cochlea to the cortex and back. Chapter 2 in: Integrative Functions in the Mammalian Auditory Pathway, Volume 15, Editors: Donata Oertel, Richard R. Fay, Springer New York, 2002.

Squire, Larry R.

2004 Memory systems of the brain: A brief history and current perspective. Neurobiology of Learning and Memory 82(3):171-177.

Stiebler, I., et al.

1997 The auditory cortex of the house mouse: Left-right differences, tonotopic organization and quantitative analysis of frequency representation. Journal of Comparative Physiology - A Sensory, Neural, and Behavioral Physiology 181(6):559-571.

Suga, Nobuo, and Xiaofeng Ma

2003 Multiparametric corticofugal modulation and plasticity in the auditory system. Nature reviews. Neuroscience 4(10):783-794.

Teich, A.H., McCabe, P.M., Gentile, C.G., Jarrell, T.W., Winters R.W., Liskowsky, D.R., Schneiderman, N.

Auditory cortex lesions prevent the extinction of Pavlovian differential heart rate conditioning to tonal stimuli in rabbits. Brain Research, Volume 480, Issues 1–2, 20 February 1989, Pages 210–218

Teich, A.H., McCabe, P.M., Gentile, C.G., Jarrell, T.W., Winters R.W., Liskowsky, D.R., Schneiderman, N.

Role of auditory cortex in the acquisition of differential heart rate conditioning. Physiology & Behavior, Volume 44, Issue 3, 1988, Pages 405–412.

Tovote, Philip, Jonathan Paul Fadok, and Andreas Lüthi

2015 Neuronal circuits for fear and anxiety. Nature Reviews Neuroscience 16(6):317-331.

Tremblay, Robin, Soohyun Lee, and Bernardo Rudy

2016 GABAergic Interneurons in the Neocortex: From Cellular Properties to Circuits. Neuron 91(2):260-292.

Ulanovsky, Nachum, et al.

2004 Multiple Time Scales of Adaptation in Auditory Cortex Neurons. J. Neurosci. 24(46):10440-10453.

Weinberger, Norman M., Hopkins W., Diamond D.M.

Physiological plasticity of single neurons in auditory cortex of the cat during acquisition of the pupillary conditioned response: I. Primary field (AI). Behav Neurosci. 1984 Apr;98(2):171-88.

Weinberger, Norman M.

2004 Specific long-term memory traces in primary auditory cortex. Nature reviews. Neuroscience 5(4):279-290.

Weinberger, Norman M.

2007 Associative representational plasticity in the auditory cortex: Resolving conceptual and empirical problems. Debates in Neuroscience 1(2-4):85-98.

Weinberger, Norman M.

2015 New perspectives on the auditory cortex: Learning and memory. Volume 129: Elsevier B.V.

Whittle, Nigel, et al.

2013 Deep brain stimulation, histone deacetylase inhibitors and glutamatergic drugs rescue resistance to fear extinction in a genetic mouse model. Neuropharmacology 64:414-426.

Wigestrand, Mattis B., et al.

2016 Primary auditory cortex regulates threat memory specificity. Learning % Memory 24:55-59.

Willott, James F., Lindsay M. Aitkin, and Sandra L. McFadden

1993 Plasticity of auditory cortex associated with sensorineural hearing loss in adult C57BL/6J mice. Journal of Comparative Neurology 329(3):402-411.

Woolf, N.J.,

Cholinergic systems in mammalian brain and spinal cord. Progress in Neurobiology

Volume 37, Issue 6, 1991, Pages 475–524

Wozny, Christian, and Stephen R. Williams

2011 Specificity of synaptic connectivity between layer 1 inhibitory interneurons and layer 2/3 pyramidal neurons in the rat neocortex. Cerebral Cortex 21(8):1818-1826.

Wu, Guangying K., et al.

2008 Lateral Sharpening of Cortical Frequency Tuning by Approximately Balanced Inhibition. Neuron 58(1):132-143.

Xu, Xiangmin, Keith D. Roby, and Edward M. Callaway

2010 Immunochemical characterization of inhibitory mouse cortical neurons: Three chemically distinct classes of inhibitory cells. Journal of Comparative Neurology 518(3):389-404.

Yassin, Lina, et al.

2010 An Embedded Subnetwork of Highly Active Neurons in the Neocortex. Neuron 68(6):1043-1050.

Yoshimura, Yumiko, Jami L. M. Dantzker, and Edward M. Callaway

2005 Excitatory cortical neurons from fine-scale functional networks. Nature 5(February):2005-2005.

Zhou, Mu, et al.

2014 Scaling down of balanced excitation and inhibition by active behavioral states in auditory cortex. Nature neuroscience 17(6):841-50.

Acknowledgements

I would like to thank Andreas for giving me the opportunity to pursue this project in his lab, for his guidance and support. I learned so much during my time here, and really appreciated the excellent scientific advice and insight.

I would like to thank Georg for providing a two-photon microscope in time of need and tons of advice. I really appreciated the opportunity to be a sort of honorary member of your lab.

A very big 'thank you' to Pawel for teaching me how to perform imaging experiments, endless patience with all my 'quick questions', and for making long imaging sessions much more fun.

Yael, thanks so much for invaluable help with analysis, and for lending an ear and giving excellent advice. I'm so happy you joined Andreas' lab!

Johannes – thank you for giving me the opportunity to work with you on your project at the beginning of my Ph.D., for great discussions and support to get my own project on the road. I have learned a lot from you.

I would like to thank my thesis committee, Botond Roska and Marlene Bartos, for advice and guidance over the years. I would also like to thank Rainer Friedrich for being the chair at my defense.

Another 'thank you' goes to the members of the Keller lab, who were the most helpful colleagues I could have wished for. Marcus, David, Alex, Ares – thank you so much for your never-ending patience!

To the 'inhabitants' of rom 4.30 – thank you! Jan, thank you for uplifting support and down-to-earth advice. Yael, thanks for being you. Nigel, thank you for your help, your advice and your friendship. Alejandro, thank you for the treats.

I would like to thank Christian, Julia, Kristine and Tobias for excellent technical support and for a lot of fun during my time here. You rock!

I would also like to thank Daniela for all the viruses I used, and for our nice conversations.

Jon and Phil – thanks a lot for your scientific advice and friendship. Another big thank you to Julien for amazing scientific advice and help. Sabine, thank you for all your help with immunos and mice.

Léma and Sol – thank you so, so much for your friendship during the last years, our trips, amazing amounts of fun, and support when the going got tough. Simon, I couldn't have done it without regular visits to the cinema. Thank you to Francois for all the philosophy. Thank you to all the members of the Lüthi lab for the great atmosphere, great scientific discussions, and all the support!

David T., thank you for providing me with these lovely mouse drawings. Jen, David T., Els, Rosie – thank you for everything!

A big, big thank you to Matthias M. for getting me started with Matlab and decoding, and for being endlessly patient with these data, even when you didn't have to be. Thank you!

And finally, thank you to my family, who were always supportive beyond any expectations, no matter what. I could not have done it without you.